AFFDL-TR-71-38

PARAFOIL FLIGHT PERFORMANCE

JOHN D. NICOLAIDES AND MICHAEL A. TRAGARZ

UNIVERSITY OF NOTRE DAME

TECHNICAL REPORT AFFDL-TR-71-38

JUNE 1971

Approved for public release; distribution unlimited.

AIR FORCE FLIGHT DYNAMICS LABORATORY
AIR FORCE SYSTEMS COMMAND
WRIGHT-PATTERSON AIR FORCE BASE, OHIO

70

UNCLASSIFIED
Security Classification

DOCUMENT CONTROL DATA - R & D

(Security classification of title, body of abstract and indexing annotation must be entered when the overall report is classified)

1. ORIGINATING ACTIVITY (Corporate author) University of Notre Dame Notre Dame, Indiana 46556	2a. REPORT SECURITY CLASSIFICATION UNCLASSIFIED 2b. GROUP N/A

3. REPORT TITLE

Parafoil Flight Performance

4. DESCRIPTIVE NOTES (Type of report and inclusive dates)

Final Report, April 1968 to April 1971

5. AUTHOR(S) (First name, middle initial, last name)

John D. Nicolaides and Michael A. Tragarz

6. REPORT DATE	7a. TOTAL NO. OF PAGES	7b. NO. OF REFS
June 1971	83	14

8a. CONTRACT OR GRANT NO. Contract AF33615-68-C-1459 b. PROJECT NO. 6065 6065 01 6065 01 009	9a. ORIGINATOR'S REPORT NUMBER(S) N/A 9b. OTHER REPORT NO(S) (Any other numbers that may be assigned this report) AFFDL-TR-71-38

10. DISTRIBUTION STATEMENT

Approved for public release; distribution unlimited

11. SUPPLEMENTARY NOTES N/A	12. SPONSORING MILITARY ACTIVITY Air Force Flight Dynamics Laboratory (AFFDL/FER) WPAFB, Ohio 45433

13. ABSTRACT

The steady state flight performance of the Parafoil is computed by using aerodynamic coefficient data obtained from wind tunnel tests of both small scale models ~~(50 in.^{2})~~ and full scale aspect ratio 2.0 units ~~(147 ft^2)~~. The actual free flight performance of the Parafoil is obtained from both manned ascending flights and manned jumps from aircraft. Attention is also given to the flight stability and control of the Parafoil and to its unique landing flare. The agreement between the performance predictions based on the wind tunnel data and the results obtained from actual flight tests is presented. The performance of a more advanced aspect ratio 3.0 Parafoil design is considered.

DD FORM 1 NOV 65 1473

UNCLASSIFIED
Security Classification

NOTICES

When Government drawings, specifications, or other data are used for any purpose other than in connection with a definitely related Government procurement operation, the United States Government thereby incurs no responsibility nor any obligations whatsoever; and the fact that the Government may have formulated, furnished, or in any way supplied the said drawings, specifications, or other data, is not to be regarded by implication or otherwise as in any manner licensing the holder or any other person or corporation, or conveying any rights of permission to manufacture, use, or sell any patented invention that may in any way be related thereto.

Copies of this report should not be returned unless return is required by security considerations, contractual obligations, or notice on a specific document.

*U.S. Government Printing Office: 1971 — 759-077/069

UNCLASSIFIED
Security Classification

14. KEY WORDS	LINK A		LINK B		LINK C	
	ROLE	WT	ROLE	WT	ROLE	WT
Parafoil						
Para-Foil						
Steerable Parachute						
Flexible Wing						
Hi-Glide Canopy						
Parachute						
Gliding Parachute						
Maneuverable Parachute						
Personnel Parachute						
Parachute Free Flight Testing						

UNCLASSIFIED
Security Classification

PARAFOIL FLIGHT PERFORMANCE

JOHN D. NICOLAIDES AND MICHAEL A. TRAGARZ

FOREWORD

This report was prepared by the University of Notre Dame, Notre Dame, Indiana, under U.S. Air Force Contract AF33615-68-C-1459. This contract was initiated under Project 6065, "Performance and Design of Deployable Aerodynamic Decelerators", Task 606501, "Terminal Descent Deceleration Concepts". The work was administered under the direction of the Recovery and Crew Station Branch of the Air Force Flight Dynamics Laboratory at Wright-Patterson Air Force Base, Ohio. Mr. S. Metres and Mr. R. Speelman served as successive project engineers during the duration of the effort.

The authors, of the University of Notre Dame Aerospace and Mechanical Engineering Department, were J. D. Nicolaides, Professor and M. A. Tragarz, Graduate Student. Contributing students of the University of Notre Dame Aerospace and Mechanical Engineering Department were Barney Goren, John Dunlop, Patrick Sullivan, Robert Hengstebeck, and Michael Higgins.

The University of Notre Dame wishes to acknowledge the contributions of Major Gerrell Plummer and the U. S. Army Golden Knights at Ft. Bragg, North Carolina and also the University of Dayton Research Institute, Dayton, Ohio.

The manuscript for this report was released by the authors in April 1971 for publication as an AFFDL Technical Report.

Publication of this report does not consitute Air Force approval of the reports findings or conclusions. It is published only for the exchange and stimulation of ideas.

GEORGE A. SOLT, JR.
Chief, Recovery and Crew Station Branch
Vehicle Equipment Division
AF Flight Dynamics Laboratory

ABSTRACT

The steady state flight performance of the Parafoil is computed by using aerodynamic coefficient data obtained from wind tunnel tests of both small scale models (50 $in.^2$) and full scale aspect ratio 2.0 units (147 ft^2). The actual free flight performance of the Parafoil is obtained from both manned ascending flights and manned jumps from aircraft. Attention is also given to the flight stability and control of the Parafoil and to its unique landing flare. The agreement between the performance predictions based on the wind tunnel data and the results obtained from actual flight tests is presented. The performance of a more advanced aspect ratio 3.0 Parafoil design is considered.

CONTENTS

LIST OF FIGURES

NOMENCLATURE

A	area (feet^2)
AR	aspect ratio (span /chord)
C_D	drag coefficient
C_L	lift coefficient
D	drag force (pounds)
F_x	force in x direction (pounds)
F_z	force in z direction (pounds)
g	acceleration of gravity (32.2 ft/sec^2)
h	altitude (feet)
I	moment of inertia about pitch axis (slug-feet^2)
L	lift force (pounds)
L/D	lift to drag ratio
m	mass (slugs)
M	pitch moment (pound-feet)
ND 2.0 (360)	Designates Notre Dame Parafoil of aspect ratio 2.0 and area of 360 sq.ft.
R	resultant aerodynamic force in z direction (pounds)
R_{ss}	steady state aerodynamic force (pounds)
Range	horizontal distance along flight path (feet)
t	time (seconds)
u	horizontal velocity (ft/sec)
V	total velocity (ft/sec)
w	vertical velocity (rate of sink) (ft/sec)
W	weight (pounds)
W/A	wing loading (pounds/ft^2)
x,y,h	down range, cross range, and altitude coordinates (feet)
x,z	Parafoil performance coordinates (feet)
α	pitch angle of attack (degrees or radians)
α_T	steady state angle of attack
γ	glide angle (degrees or radians)
ρ	density of air (slugs/ft^3)

INTRODUCTION

The Parafoil* is an aircraft or glider which can be packed and deployed like a parachute. It is made of nylon cloth, and is completely non-rigid. When in flight it takes the form of a rigid flying wing. The first aerodynamic data from wind tunnel tests and from flight tests was reported at the 1st AIAA-Aerodynamic Deceleration Systems Conference [1] and in Ref. 2. Progress in applying the Parafoil to various aeronautical applications [3-7] was summarized at the 2nd AIAA Aerodynamic Deceleration Systems Conference. [8] A review of aircraft type applications is given in Ref. 10. The flight performance of the Parafoil will be summarized in this report.

Since the Parafoil is both an airplane or glider and also a parachute or decelerator, both aircraft and decelerator type flight tests have been carried out to evaluate the performance of the Parafoil. These various flight tests include Ground Tow, Ascending Flights, and Jumps, Figs. 1-3.

Based on the aerodynamic stability coefficient data as obtained from the various wind tunnel tests, [11] the steady state flight performance of the Parafoil has been computed over a wide range of flight angles of attack ($-8^{\circ} < \alpha < +80^{\circ}$) and over a wide range of wing loadings ($.5 \leq W/A \leq 5$).

During the validating full scale free flight tests of this report attention was given to steady state flight, flight stability and control, and the unique landing flare of the Parafoil.

Extensive kite tests [2,5], unguided drop tests [9], guided drop tests, (payload recovery [4] and cargo [6]), and ground tow tests [5], Fig. 1, have been carried out. The experimental data on Parafoil flight performance used in this report was obtained from ascending flights, Fig. 2, carried out at Wright-Patterson AFB and from special jumps, Fig. 3, carried out at Wright-Patterson AFB and at the University of Notre Dame.

The landing flare maneuver allows the Parafoil to be landed like a bird with near zero forward velocity and near zero vertical velocity. A theory of motion for the flare maneuver is programed for computer prediction and is compared with the experimental flight tests.

The predicted flight performance of Parafoils of higher aspect ratio and higher wing loading is given in the Appendix.

---

*The Parafoil is a design and development of Dr. John D. Nicolaides "patent pending" and is based on the multi-cell ram airfoil Patent No. 3285546 held by SRRC, Inc., Florida.

PARAFOIL PERFORMANCE THEORY

Equations of Motion

The equations of motion for Parafoil flight are given by,

$$\sum F_x = m\dot{u} = L \sin\gamma - D\cos\gamma \tag{1}$$

$$\sum F_z = m\dot{w} = -R + mg \tag{2}$$

$$\sum M = I\ddot{\theta} \tag{2a}$$

$$L \equiv C_L \frac{1}{2} \rho V^2 A \quad \text{(Fig. 4)} \tag{3}$$

$$D \equiv C_D \frac{1}{2} \rho V^2 A \tag{4}$$

$$C_L = C_L(\alpha) \tag{5}$$

$$C_D = C_D(\alpha) \tag{6}$$

$$R_{ss} = \sqrt{L^2 + D^2} \tag{7}$$

The steady state flight velocity is obtained by setting Eq. (2) equal to zero and substituting Eqs. (3)-(7) as

$$V = \sqrt{\frac{2\,(W/A)}{\rho C_L \sqrt{1+\left(\frac{1}{L/D}\right)^2}}} \tag{8}$$

The rate of sink is given by

$$w = V \sin\gamma \tag{9}$$

The glide angle is given by Eq. (1) as

$$\gamma = \cot^{-1} (L/D) = \tan^{-1} \frac{w}{u} \tag{10}$$

Aerodynamic Coefficient Data

Extensive wind tunnel tests on various Parafoils have been carried out.[11] Representative wind tunnel data for a Parafoil of aspect ratio two is given in Fig. 5.[8,10,11] Additional wind tunnel data exists on Parafoils having aspect ratios of .5, 1.5, 2.5, and 3. Rigid, semi-rigid, and completely non-rigid wind tunnel models have been tested.

Parafoil Performance Predictions

Utilizing the wind tunnel data of Fig. 5 for an aspect ratio 2.0 Parafoil and the basic equations of motion, the steady state flight performance of the Parafoil has been computed. For example, in Fig. 6 the total velocity, the horizontal velocity, and the vertical velocity of the Parafoil are given over a range of angles of attack from -8° to 80° for a wing loading of one. It is noted that the lowest sink rate occurs near the angle of attack for the best L/D value.

In Figs. 7-9, the various flight velocities are given for wing loadings ranging from .5 to 5 for an aspect ratio 2 Parafoil.

PARAFOIL ASCENDING FLIGHTS

The Parafoil was first tested as a kite where its flight stability and aerodynamic efficiency, L/D, could be observed.[1,2] However, the variations in the wind made accurate measurements difficult. When the wind was light, a tow car was used. Fig. 2. When the tow car was stopped, the Parafoil would glide stably back to earth. Fig. 10. Ribbons and small parachutes were tied to the payload in order to provide a measure of the glide angle. Subsequent ascending and glide tests utilized smoke for the measurement of lift-to-drag ratios.[8] As on board instrumentation increased, special flight carts were constructed. The flight measurements included total velocity, rate of sink, vertical glide angle and on board movies.

During the early kite tests of large Parafoils (165 ft^2, 300 ft^2, and 360 ft^2), it was not unusual for students to be lifted into the air. Thus, when the flight test carts were available, it became possible to carry out the first manned ascending flights.[7,8,10,12] The purpose of these ascending flights was to investigate Parafoil performance and controllability and to study the unique landing flare maneuver. The simplicity and safety of these ascending cart flights led to the elimination of the cart and to direct manned ascending flights.

Ascending Flight Test Procedures

The ascending flight testing technique is illustrated in Fig. 11. The flier wears a standard jump harness with special tow harness and release. Fig. 11a. A tow line is tied to the tow vehicle. Fig. 2. When the launch team is ready and suitable commands are provided by radio, the tow vehicle moves forward. The two wing men assist in inflating the Parafoil and in providing a coordinated release. Fig. 11b. The flier upon leaving the ground ascends smoothly to altitude (500 ft to 1000 ft). Fig. 11c. When he is nearly overhead, a signal is given to him to release himself. He then glides stably to earth.[11] At an altitude to approximately 6 ft., he is given a signal to flare out thus reducing both his forward velocity and his vertical velocity to near zero. Fig. 12.

Ascending Flight Results

Numerous manned ascending flights have been carried out, the most extensive of which were those carried out in April and August of 1969 at Wright-Patterson AFB under the direction of Air Force Flight Dynamics Laboratory.

In these Air Force-Notre Dame tests, two phototheodolites were used to determine the three position coordinates, x-down range, y-cross range, and h-altitude. By differentiating this position data, values are obtained for the horizontal velocity, the total velocity and the sink rate. Representative data reduced by University of Dayton are given in Fig. 13. Values are also estimated for the lift to drag ratio; however, it can be seen from Fig. 13b that the data is quite oscillatory.

Figure 13a illustrates a typical up wind flight (Wind 4 mph). Fig. 13b is a down wind (Wind 7 mph) flight. Here the flier is towed to altitude into the wind and upon release he makes a right 180° turn and flies down wind. At the end of the flight he makes another 180° turn placing himself into the wind for his flare landing.

One of the primary purposes of the Air Force-Notre Dame tests was to determine the stability and controllability of the Parafoil. Accordingly, on certain flights, the flier executed various turns of different steepness and diameter. Plots of selected data from these maneuvering flights is illustrated in Fig. 14. Various control deflections from 1/4 to full were employed. The Parafoil is controlled by deflecting the right or the left trailing edge by pulling a control line. The area of each control surface is 1/2 b x 1/4 c, which is 25 ft^2 for the 200 ft^2 Parafoil, ND 2.0 (200). The exact angle of control deflection is difficult to determine. Full deflection is 90°; thus 1/4 deflection is 25°, etc. Following aircraft practice the path of the center of gravity defines the turn. In view of the light weight of the Parafoil (12lbs), the center of gravity of the Parafoil plus flier system is taken to be at the flier. As seen in the ground tracks of Fig. 14, when the effects of wind drift are removed, turn circle diameters of 50 ft to 400 ft were obtained. This represents good aircraft performance in view of the fact that the span of the Parafoil ND 2.0 (200) is 20 ft. During these maneuvering flights, the Parafoil exhibited excellent flight stability.

In order to provide an indication of the average flight performance, the reduced data was punched on IBM cards. The results obtained from computer averaging are given in Table I.

Flare Maneuver

One of the most impressive features of the Parafoil is its ability to land like a bird. On landing the flier heads into the wind. His nominal forward velocity is 25.6 MPH and his rate of sink is 10.5 ft/sec., Fig. 3. When he reaches an altitude of approximately 20 ft * he begins to pull down on both

*An experienced flier who commands his own flight normally initiates the flare maneuver at an altitude approximately 20 ft by slowly pulling down both control lines so as to program C_L and C_D in a near optimum manner.

control lines. Approximately 3 seconds later his hands are down to his knees and the entire trailing edge of (bx $\frac{1}{4}$ c) of the Parafoil is fully deflected ($\delta_E \approx 90^o$). The Parafoil appears to come to a complete stop in the air and the flier simply steps down lightly on one foot. Figs. 12a and 12b.

One of the purposes of the Air Force/Notre Dame Parafoil Flight Test Program was to measure and to compute this unique flare maneuver. Flight data on Parafoil total velocity and sink rate during the flare maneuver is given in Fig. 15a. In Figure 15b the flare maneuver data in flights 609, 605, and 633 have been normalized to steady state flight conditions of $V = 40.5$ ft/sec and $w = 12.02$ ft/sec.*

The equations of motion for transient flight are given by Eq. (1), (2), and (2a). These equations were coded for computer (Univac 1107) integration using programed C_L and C_D aerodynamic data. The agreement between the flight data and the computer integration of the equations of motion are given in Fig. 15b and are itemized in Table II where it is seen that a substantial reduction in flight velocity and in rate of sink are obtained.**

*These conditions are representative of the final phase of the ascending flight tests. The differences from nominal Parafoil steady state flights are due to pilot anticipation and minor controlling.

**These data reproduce the flight performance and agree with the wind tunnel data for flap deflection except for the last four steps which were extrapolated.

PARAFOIL JUMP FLIGHTS

Seven jump flight tests were carried out at the Air Force Flight Dynamics Laboratory by the University of Notre Dame in conjunction with the U. S. Army Golden Knights. Excellent flights were obtained with jump training Parafoil ND 2.0 (360), Fig. 16b. However, due to the high winds and the runway thermals, abnormally high values of L/D were obtained.

Parafoil ND 2.0 (242) jump flight tests have been carried out by the U.S. Army[13,7], (approximately 500+) Fig. 16a. Approximately 180 Parafoil ND 2.0 (200) jump flight tests have been carried out by the University. In these Notre Dame tests a Magnus rotor was used to measure total flight velocity; a rate of sink aircraft instrument was used to measure vertical velocity; altitude and time of flight were recorded in the aircraft; smoke was used to measure glide angle, and motion pictures of the deployment and flight were taken. From these flights ($W/A \approx 1.0$) representative values were obtained for the rate of sink (11 ft/sec) and the total velocity (29 MPH). On these jumps the deployment bag and two pilot parachutes are attached to the Parafoil so as not to loose them. When this extra drag was cut away, the flight velocity increased (31 MPH) and the rate of sink decreased (10 ft/sec). By measuring the smoke angle, lift to drag ratios in excess of 5 have been consistently obtained. For additional lift-to-drag ratio values see Ref. 8 and 9.

PERFORMANCE ESTIMATION

Ascending Flights

Various Parafoil ascending flights have been carried out, some straight, some turning, and some with intentional pitching disturbance, Table I.* It is noted that the straight and longer flights better permit the Parafoil to reach steady state flight performance. Of the quantities measured from these flight tests, the best determined is the rate of sink since it is relatively insensitive to wind indeterminancy. A review of Table I suggests that a representative rate of sink** for the ND 2.0 (200) is approximately 10.5 ft/sec., for the ND 2.0 (360) is approximately 6.5 ft/sec., and for the ND 2.0 (242) is approximately 8.0 ft/sec. Representative values for horizontal velocity are difficult to determine because of wind changes and inaccuracy of wind measurement. It is suggested by Table I that the horizontal velocity for ND 2.0 (200) may be 36 ft/sec, for ND 2.0 (360) may be 24 ft/sec, and for ND 2.0 (242) may be 30 ft/sec. A summary is provided in Table III. Measurements of the flight angle of attack of the Parafoil were found difficult to obtain. However measurements from the sequence still photographs of the flight angle of attack of ND 2.0 (200) were found to be approximately 3^{o}.

Jump Flights

The representative quantities measured in the jump flights were given previously and are also summarized in Table III. The measurements of total velocity are considered quite good. The values for rate of sink are approximate. The values for the lift to drag ratio are considered good since they are obtained from smoke tracks of steady state flight over long observation times, Figure 3.

*The data in Table I was obtained by computer averaging all of the AF/Dayton University Parafoil data for each flight. All transient as well as steady state data is included.

**For Parafoil ND 2.0 (200) flights 604, 608, and 611 were used since they were of long duration and therefore allowed the Parafoil to reach steady state performance. For Parafoil ND 2.0 (360) flight 630 was used because of its long duration. For Parafoil ND 2.0 (242) flights 625 and 627 were used because of their long duration.

COMPARISON OF PREDICTED AND MEASURED PARAFOIL PERFORMANCE

It is now possible to compare the predictions of Parafoil flight performance, Figures 5-9, with the actual measured Parafoil flight performance as obtained on the Standard Jump Parafoil, ND 2.0 (200), and on the Training Jump Parafoil, ND 2.0 (360). This comparison may begin by considering the measured rate of sink for Parafoil ND 2.0 (200) which is 10.5 ft/sec. Entering Fig.9 or Fig.17b with this rate of sink and using the curve prepared for a wing loading of one, we find a predicted angle of trim of approximately 3°. The angle of trim measured from the sequence stills of actual flight was approximately 3°. Thus there is good agreement between the measured value and the predicted value of trim as obtained from Figure 17b using the measured rate of sink.

A comparison between predicted total velocity and measured total velocity may be obtained by using Figure 7 or Figure 17c. By entering Figure 17c with an angle of trim of 3° we obtain a value of the predicted total velocity of approximately 38 ft/sec. The value of the total velocity from the ascending and glide tests is 37.6 ft/sec, $\sqrt{(36^2 + 10.5^2)}$, and from the jump tests is 42.5 ft/sec. The agreement between the predicted total velocity and the value obtained from the ascending flights is quite good. However, the measured jump value is high.

A comparison between the wind tunnel measured lift-to-drag ratio and flight measured lift-to-drag ratio may be obtained by considering Figure 5 or Figure 17a where for a trim of 3° we obtain a value of 3.8. The value of lift-to-drag ratio measured in the ascending and glide flight tests was 3.4 and in the jump tests was 3.7. (See Table III). The ascending flight value is low. However, as mentioned previously, the wind correction is uncertain as is the measured α_T.

The agreement with the jump value is misleading since the jump units carried considerable extra drag due to two pilot parachutes and the deployment bag which are all tied to the trailing edge of the Parafoil. As indicated in Table III, the lift-to-drag ratio increases to 4.4 when this extra drag is removed. Also, the jump unit is trimmed at a larger angle of attack which accounts for their improved lift-to-drag ratio which agrees quite well with the wind tunnel value for best trim. Figure 17a.

Figures 17a-17d also contain similar performance comparisons for Parafoil ND 2.0 (360). In general the agreement between the predicted and the measured performance for both Parafoils is good.Thus the Parafoil performance curves given herein should prove useful to designers in considering the application of Parafoils to various missions and requirements. Excellent flare agreement is illustrated in Figure 15b.

FLIGHT PERFORMANCE OF ADVANCED PARAFOIL DESIGN

The first multi-cell kites (Falcon and Hawk)[1,11] had an aspect ratio of approximately 1/2 and 1. The first Parafoil had an aspect ratio of 2.0. Since most Parafoil studies and tests had been carried out on the aspect ratio 2.0 units, it was decided to use nominal AR=2 units in the various application programs which arose. The flight tests carried out under this current program also used aspect ratio 2.0 units. (A=147, 200, 242, and 360 ft^2.) Wind tunnel tests, however, have been carried out on Parafoil designs having aspect ratios of .5, 1.0, 1.5, 2.0, 2.5, and 3.0. Thus, since the comparison of the predicted and the measured flight performance on the aspect ratio 2 Parafoil was good, it is of special interest to consider the predicted flight performance of the other units. These calculations of flight performance of various Parafoil designs are given in the Appendix.

The flight performance of Parafoil ND 3.0 (200) with a wing loading of one, Fig. I-24, is of special interest when compared with Parafoil ND 2.0 (200).

	L/D	V	w	α_T
ND 2.0 (200)	4.6	32.6	6.9	8^o
ND 3.0 (200)	6.5	30	4.6	6^o

Thus, by using a Parafoil of aspect ratio 3.0 the total flight velocity and the rate of sink are reduced and the glide distance is improved.

CONCLUDING REMARKS

An ascending and gliding Parafoil testing technique has been developed and has been successfully utilized for the determination of steady state flight performance data. Both straight flights and turning flights have been carried out from altitudes of approximately 1000 ft. The unique landing flare maneuver has been measured and analyzed.

A technique for manned jumping the Parafoil from aircraft has been evolved and has been employed for the determination of Parafoil flight performance.

The equations of motion for steady state Parafoil flight have been developed and coded for computer computation utilizing basic Parafoil wind tunnel data. The computer runs have provided predictions of Parafoil performance for various wing loadings and trim angles.

A comparison of the predicted flight performance of the Parafoil with the measured flight performance of the Parafoil, as obtained from ascending flight and glide tests and from jump tests, has been made. The agreement between the predicted performance and the measured performance is good, and thus a designer, desiring to use the Parafoil in various applications, may with confidence employ the curves and data in the report.

The flight performance of various aspect ratio (1-3) Parafoil designs at different wing loadings (1-10) and trim angles ($-8^{o} \rightarrow 67^{o}$) is given in the Appendix.

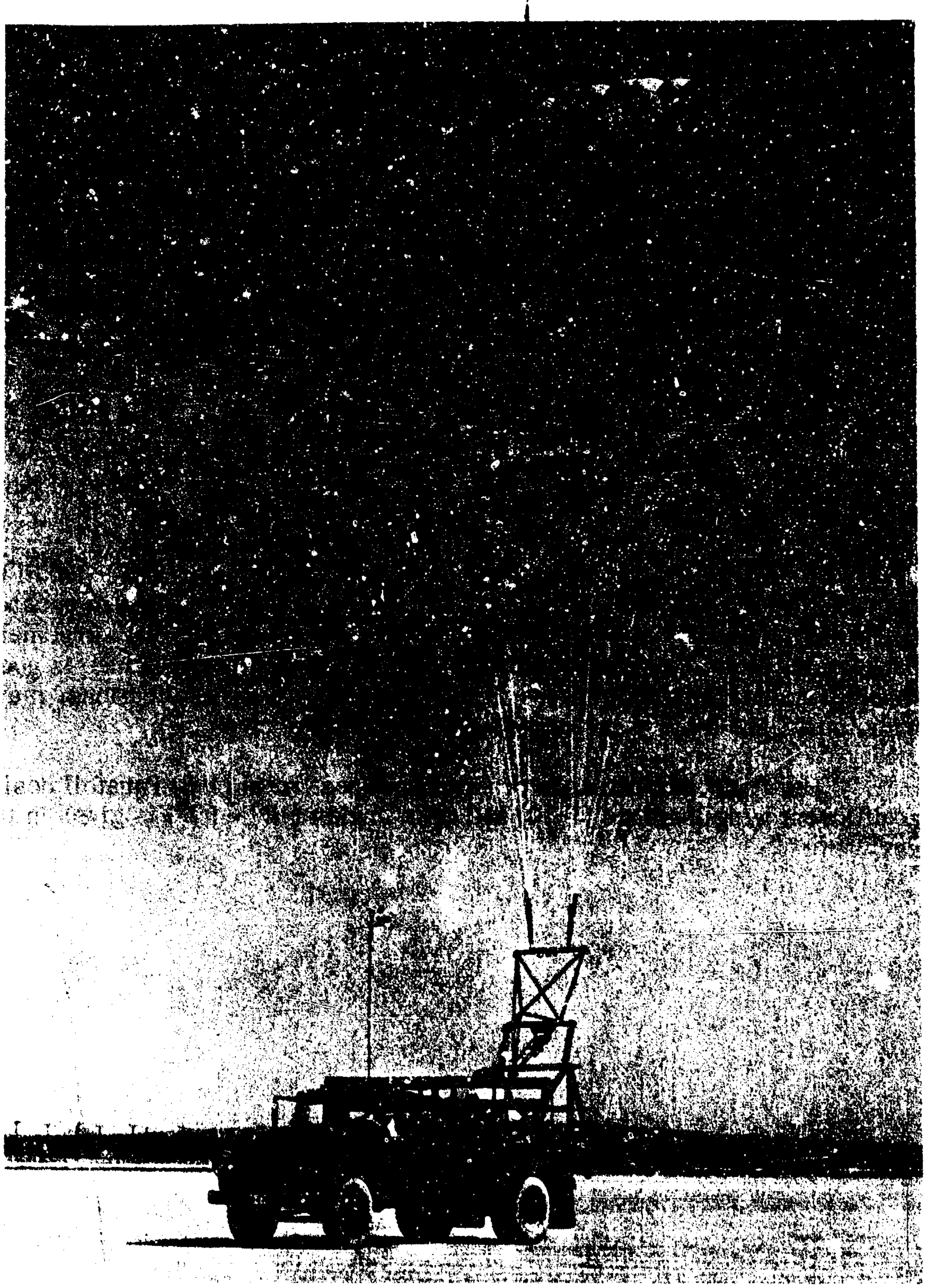

Figure 1. NASA Tow Test

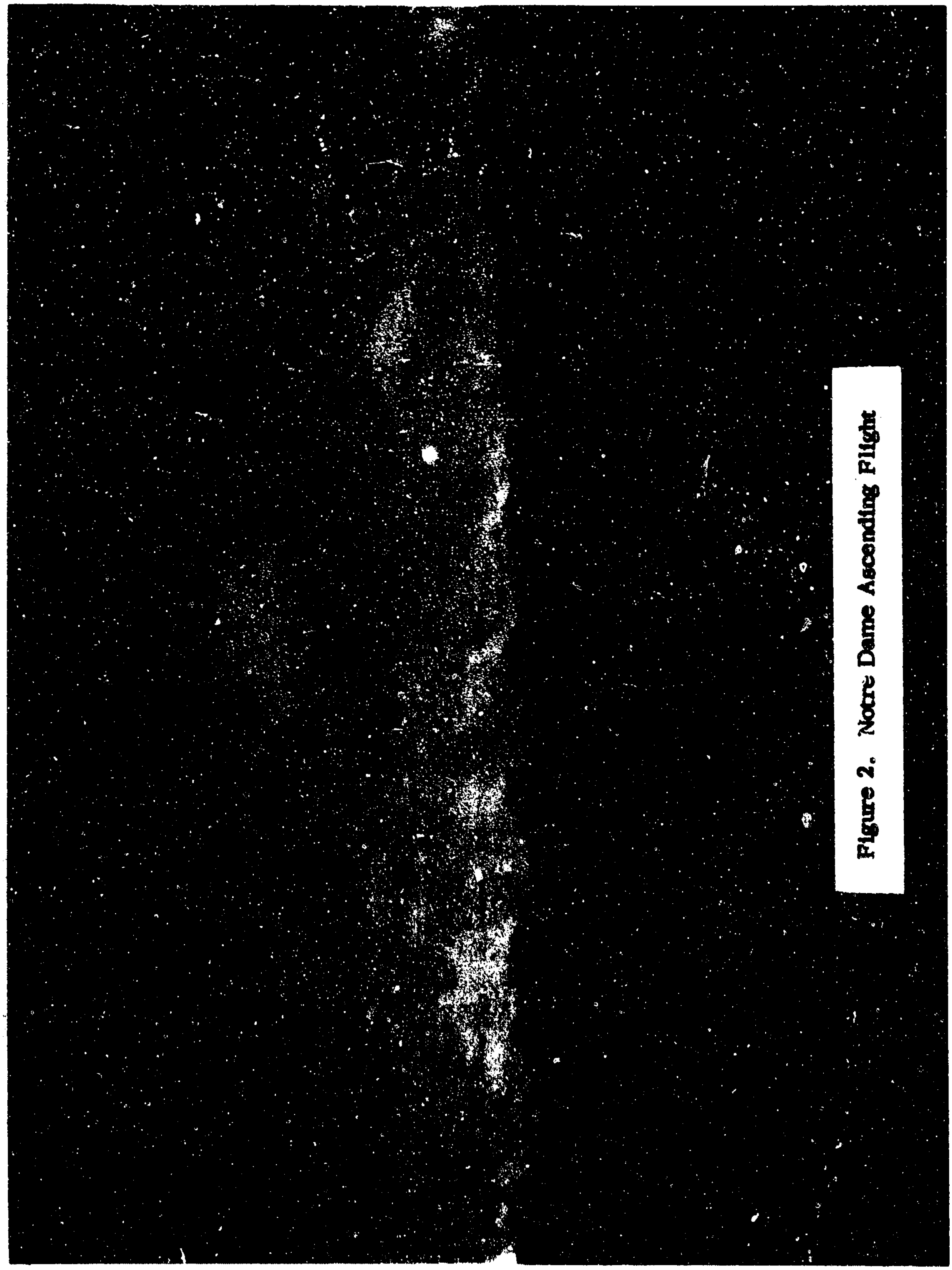

Figure 2. Notre Dame Ascending Flight

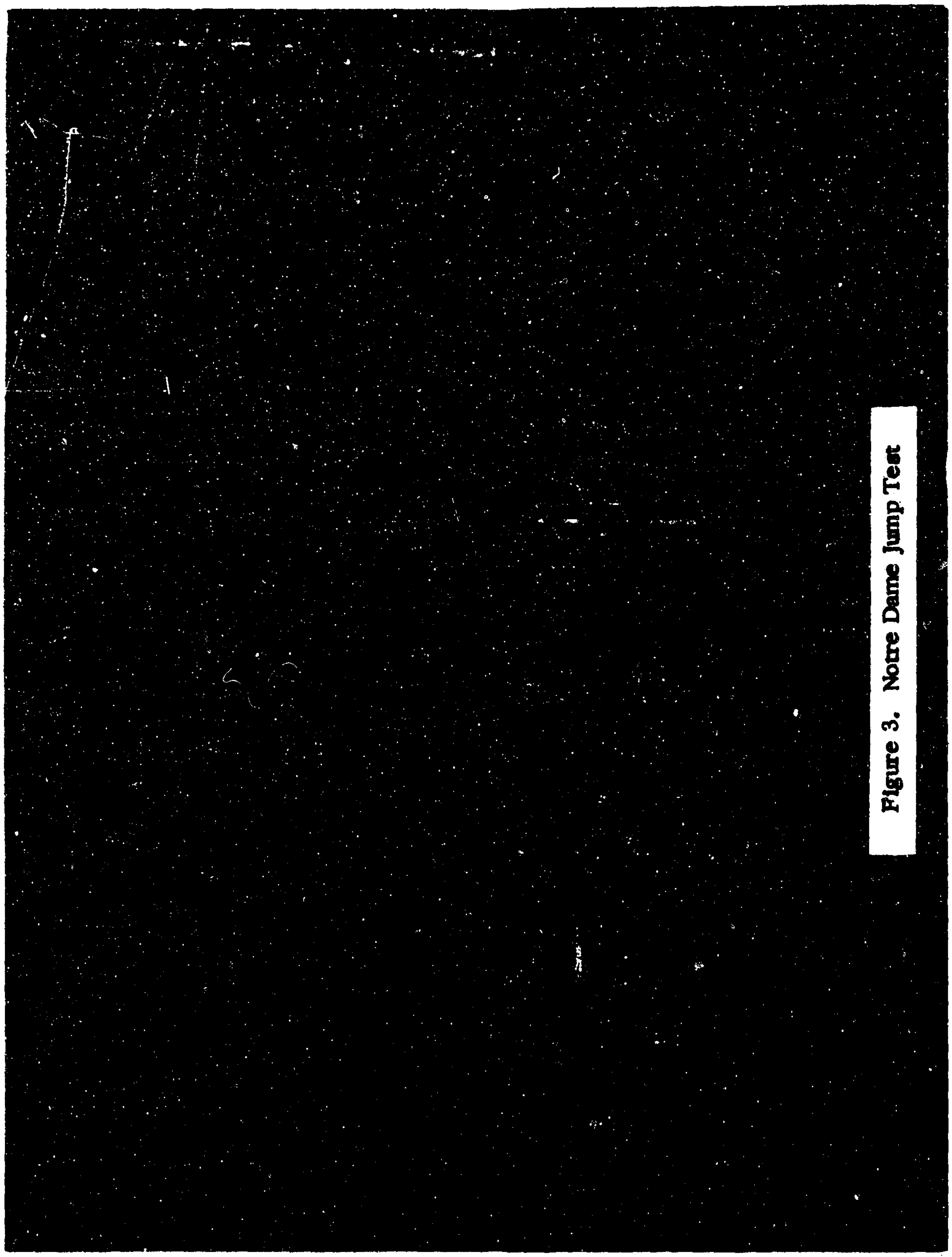

Figure 3. Notre Dame Jump Test

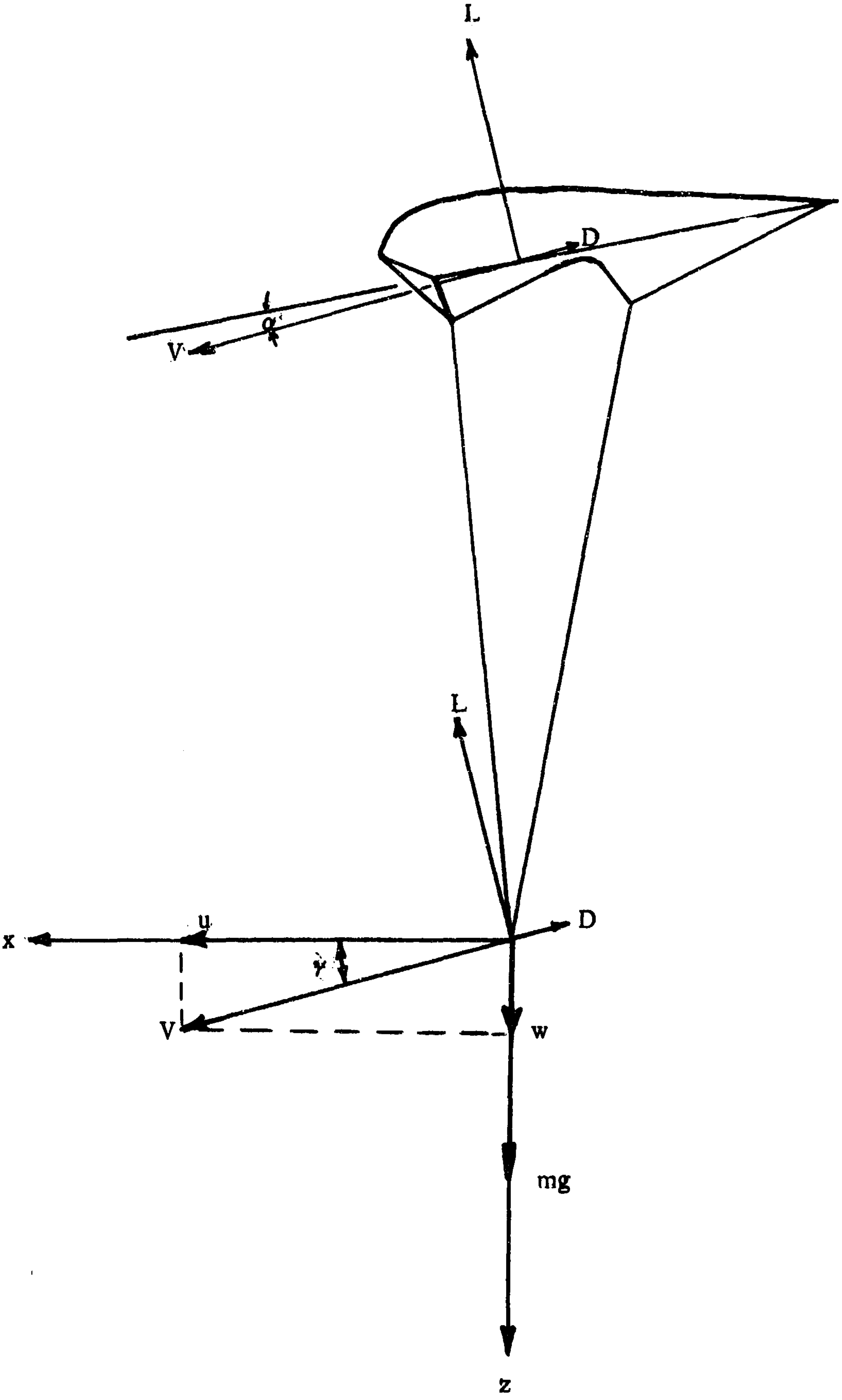

Figure 4. Flight Dynamic System

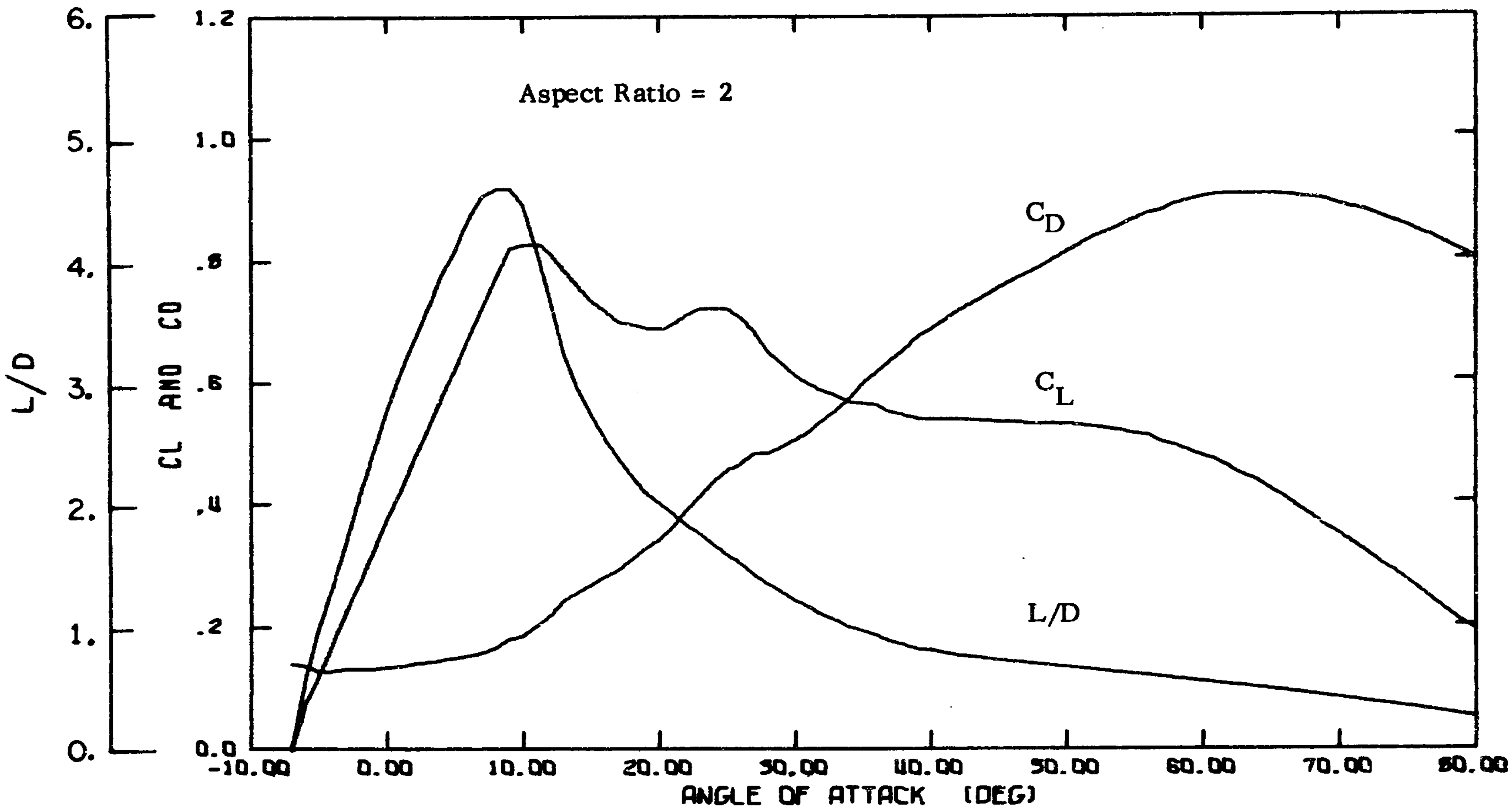

Figure 5. Parafoil Aerodynamic Data, Aspect Ratio = 2

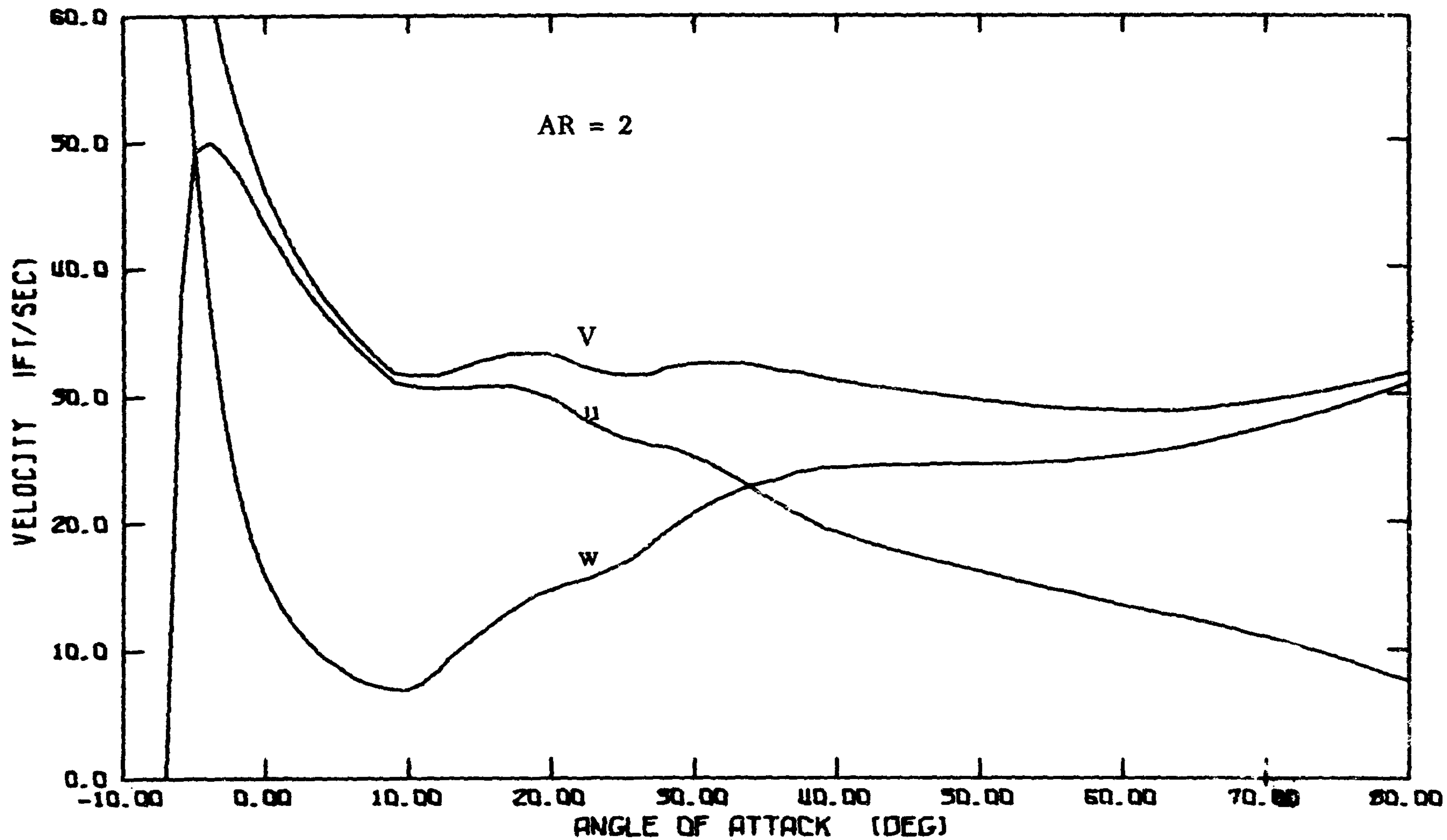

Figure 6. Parafoil Flight Velocities. Wing Loading = 1

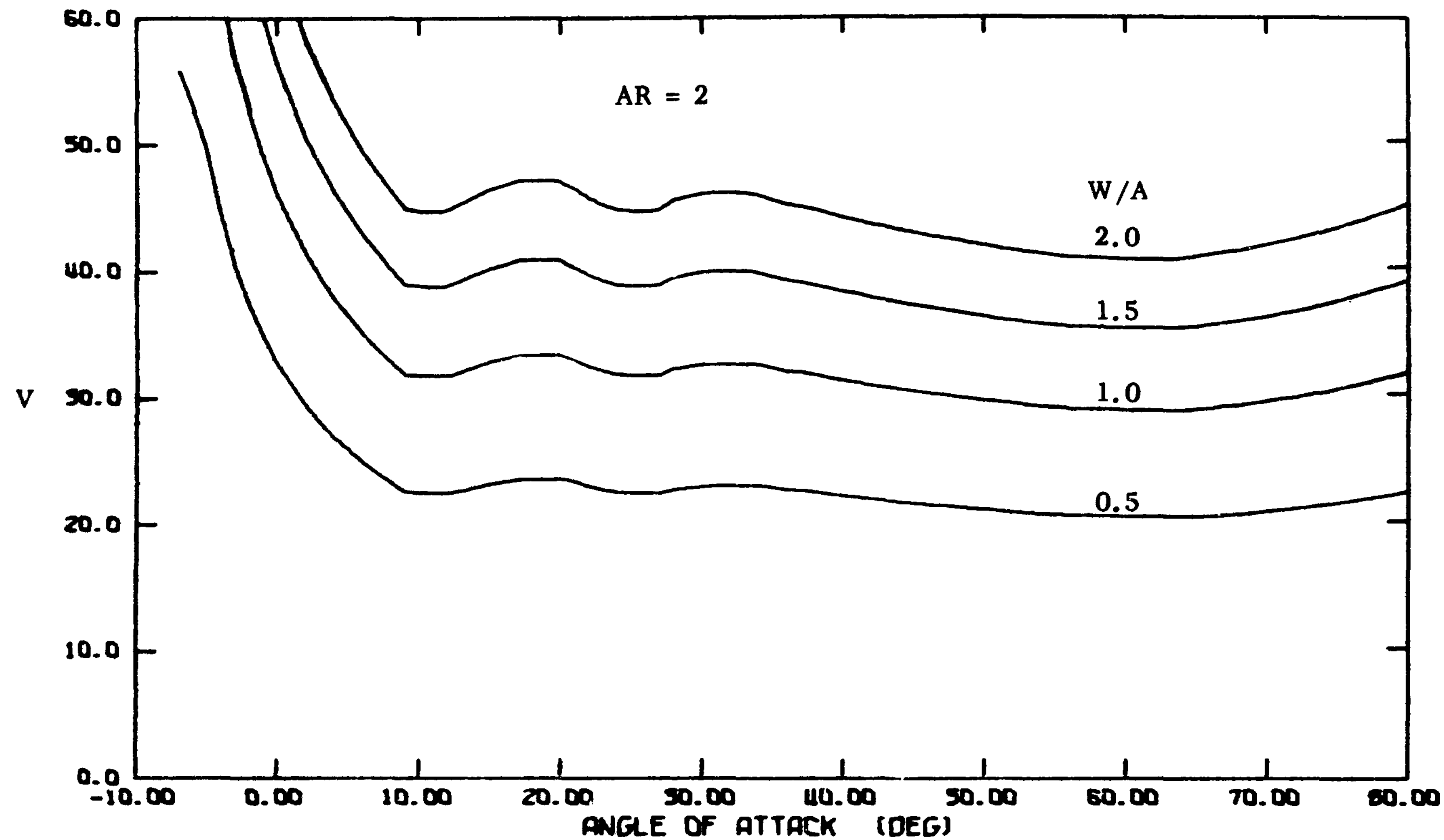

Figure 7. Parafoil Flight Velocity

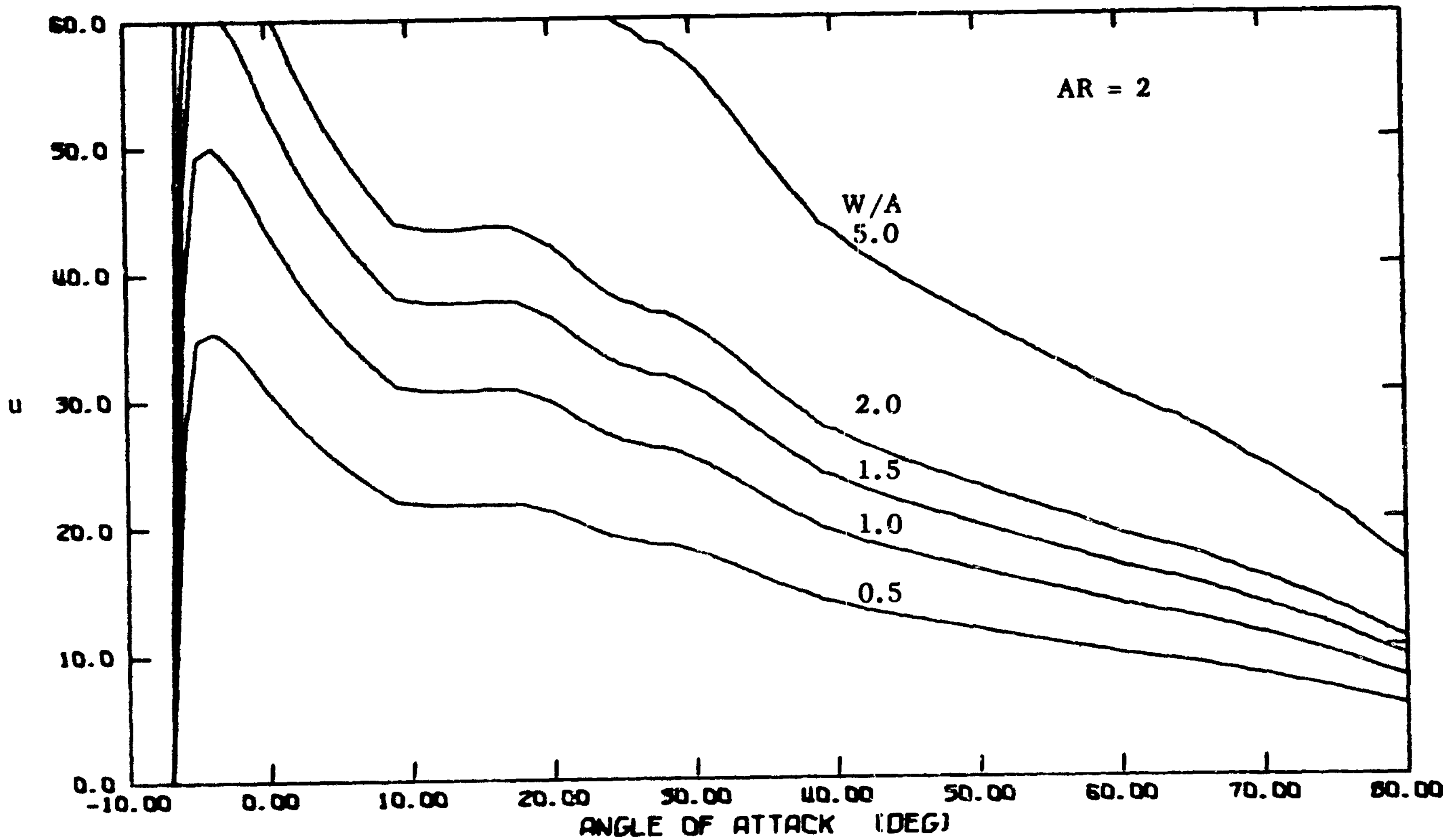

Figure 8. Parafoil Horizontal Velocity

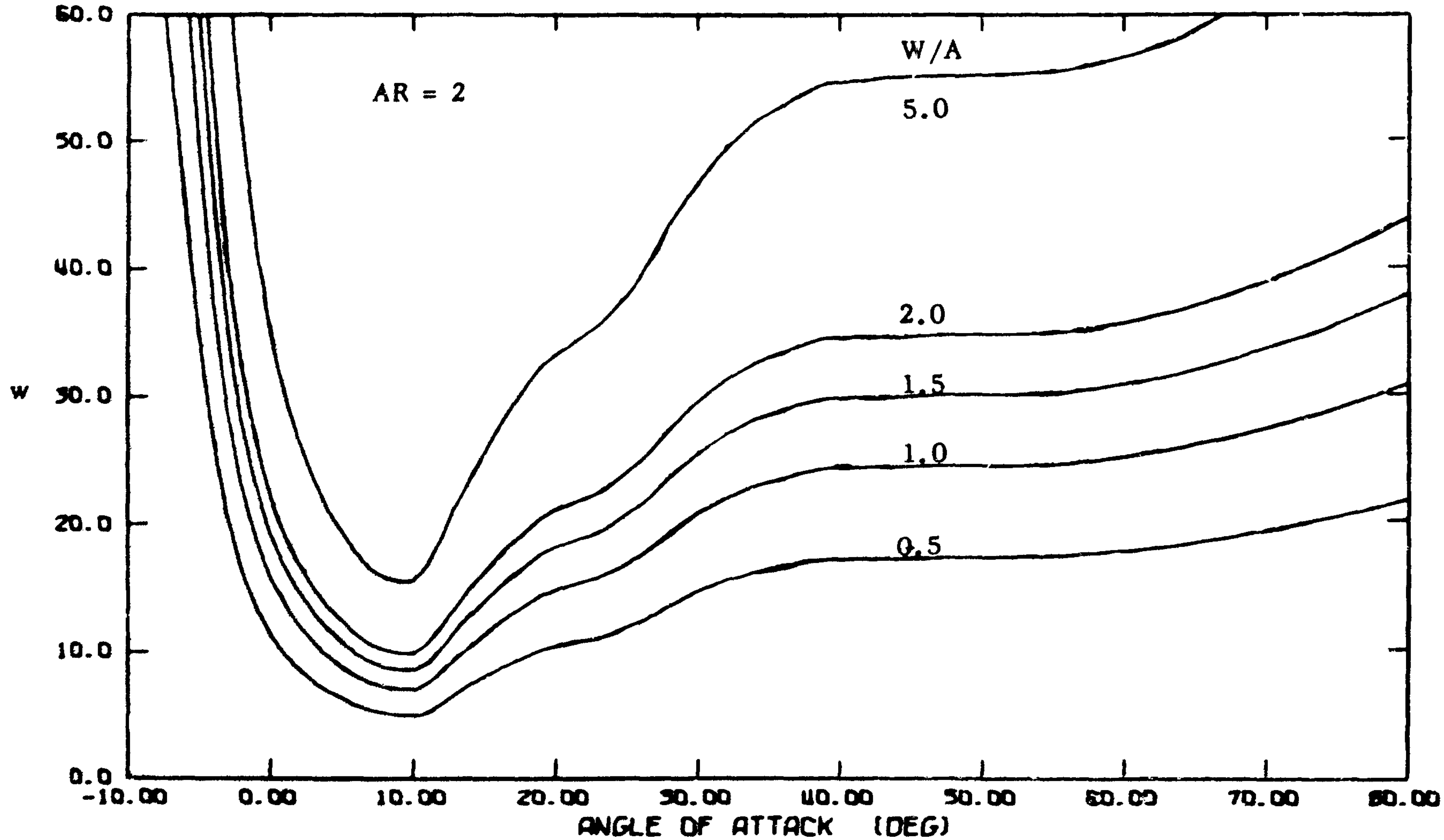

Figure 9. Parafoil Vertical Velocity

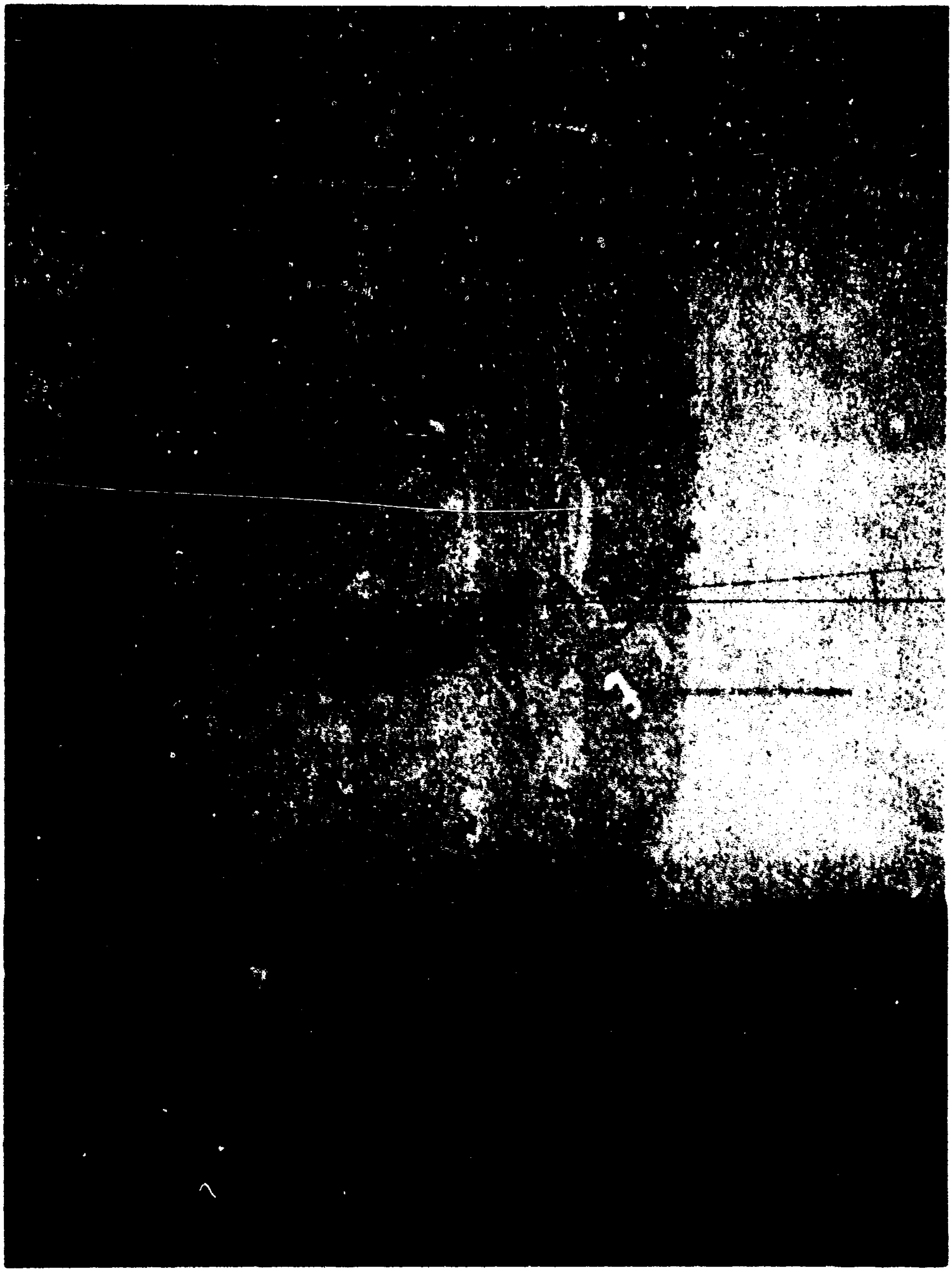

Figure 10. Air Force 2000# Cargo Parafoil, A=864.

Figure 11a. Boeing Chief Test Pilot, Dale Felix

Figure 11b. Start of Tow

Figure 11c. Manned Ascending Flight

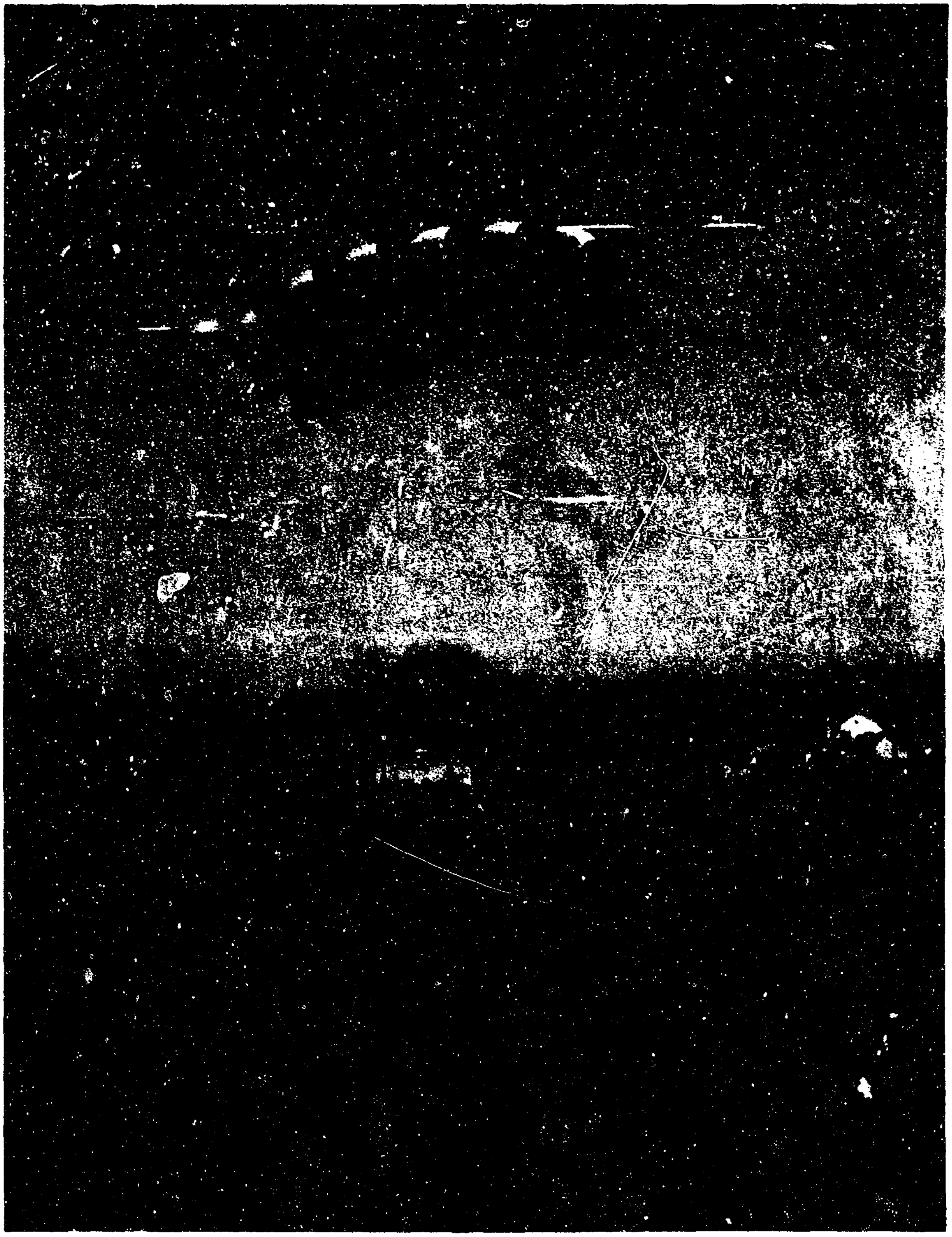

Figure 12a. Flare Landing

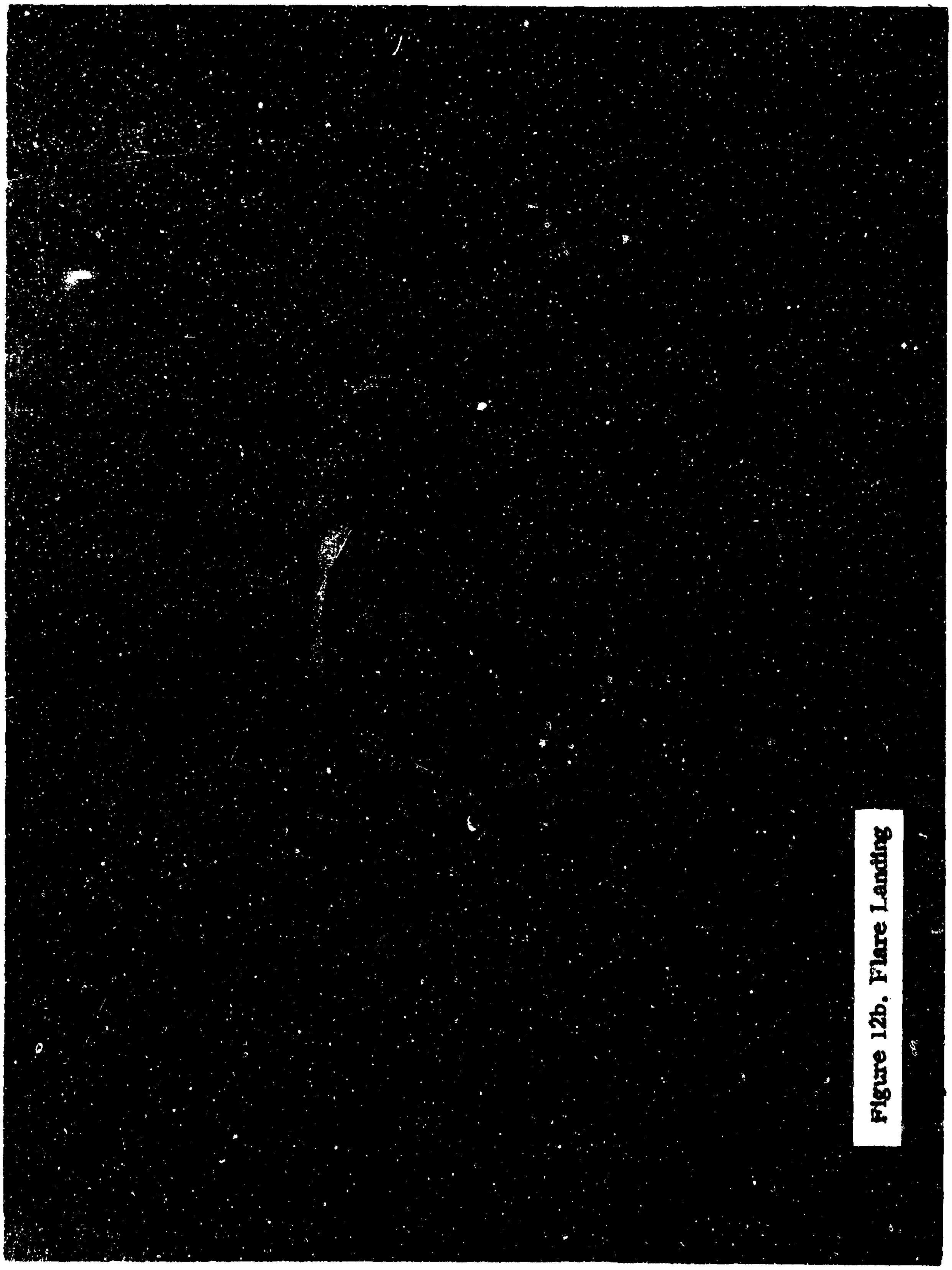

Figure 12b. Flare Landing

TABLE I

ASCENDING FLIGHT DATA

(Low α_T)

Flight	Duration (sec)	V (ft/sec)	u	w	L/D	A (ft^2)	Flight Type
603	44.7	35.4	32.7	13.0	2.7	200	St.
604	50.7	33.2	31.3	10.6	3.2	200	St.
605	51.5	30.7	27.9	12.6	2.4	200	St.
606	42.0	32.8	29.1	13.8	2.1	200	St.
607	48.5	28.1	24.3	14.0	1.9	200	St.
608	57.7	32.0	30.1	10.5	3.2	200	St.
611	59.2	36.3	34.3	10.5	4.1	200	DW
612	47.2	40.3	37.9	12.6	3.4	200	DW
613	37.7	42.9	40.4	13.7	3.0	200	DW
614	44.5	41.2	38.8	13.3	3.0	200	DW
617	59.0	36.9	34.7	12.3	2.8	200	Turns
618	46.2	32.0	28.8	13.1	2.5	200	Turns
619	42.0	38.2	34.3	15.9	2.7	200	Turns
620	39.2	35.4	31.5	15.5	2.2	200	Turns
623	45.2	35.7	32.7	13.7	2.5	200	Pitch
624	50.2	33.8	30.8	13.8	2.7	200	Pitch
625	94.7	31.3	30.1	8.0	3.9	242	DW
626	54.2	32.5	30.1	10.8	3.5	242	DW
627	73.0	29.9	28.7	7.9	4.0	242	DW
628	79.0	26.7	25.0	8.9	2.9	360	DW
629	92.2	25.1	23.8	7.5	3.5	360	DW
630	[illegible]9.0	23.8	22.8	6.0	4.1	360	DW
631	[illegible].2	36.7	34.5	12.2	2.9	200	DW/P
632	52.7	34.2	31.4	13.2	2.4	200	St/P
633	40.0	38.3	35.9	13.1	2.8	200	DW/P
634	44.5	35.4	33.1	12.2	2.7	200	St/P
636	47.7	37.9	35.3	13.6	2.7	200	DW/P

W = 185 # (200 ft^2)
W = 197# (360 ft^2)
W = 186# (242 ft^2)

St. = Straight Flight
DW = Down Wind Flight
Turns = Turning Flight
Pitch, P = Pitch Disturbance

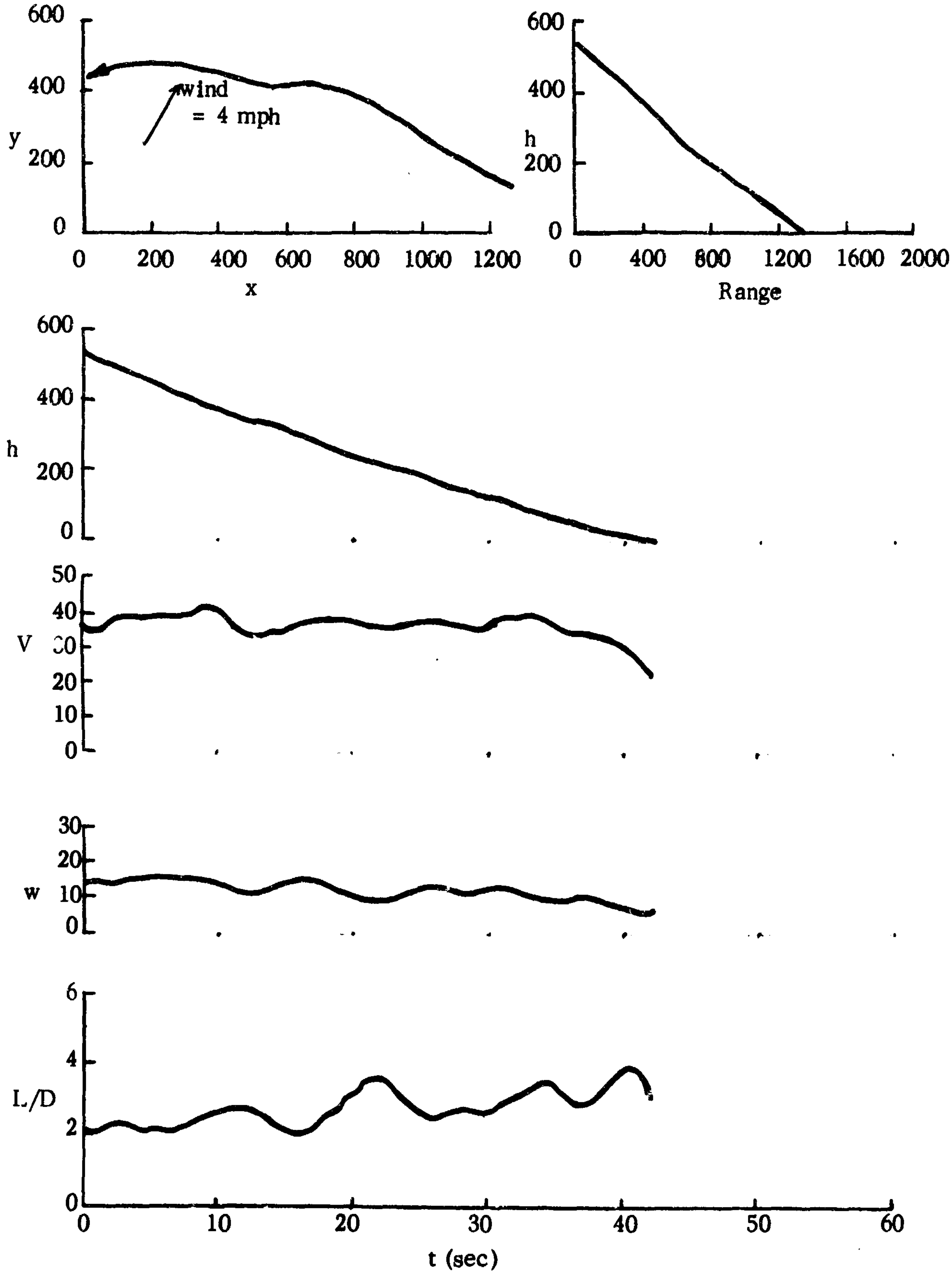

Figure 13a. Air Force Ascending Flight Data (634) University of Dayton

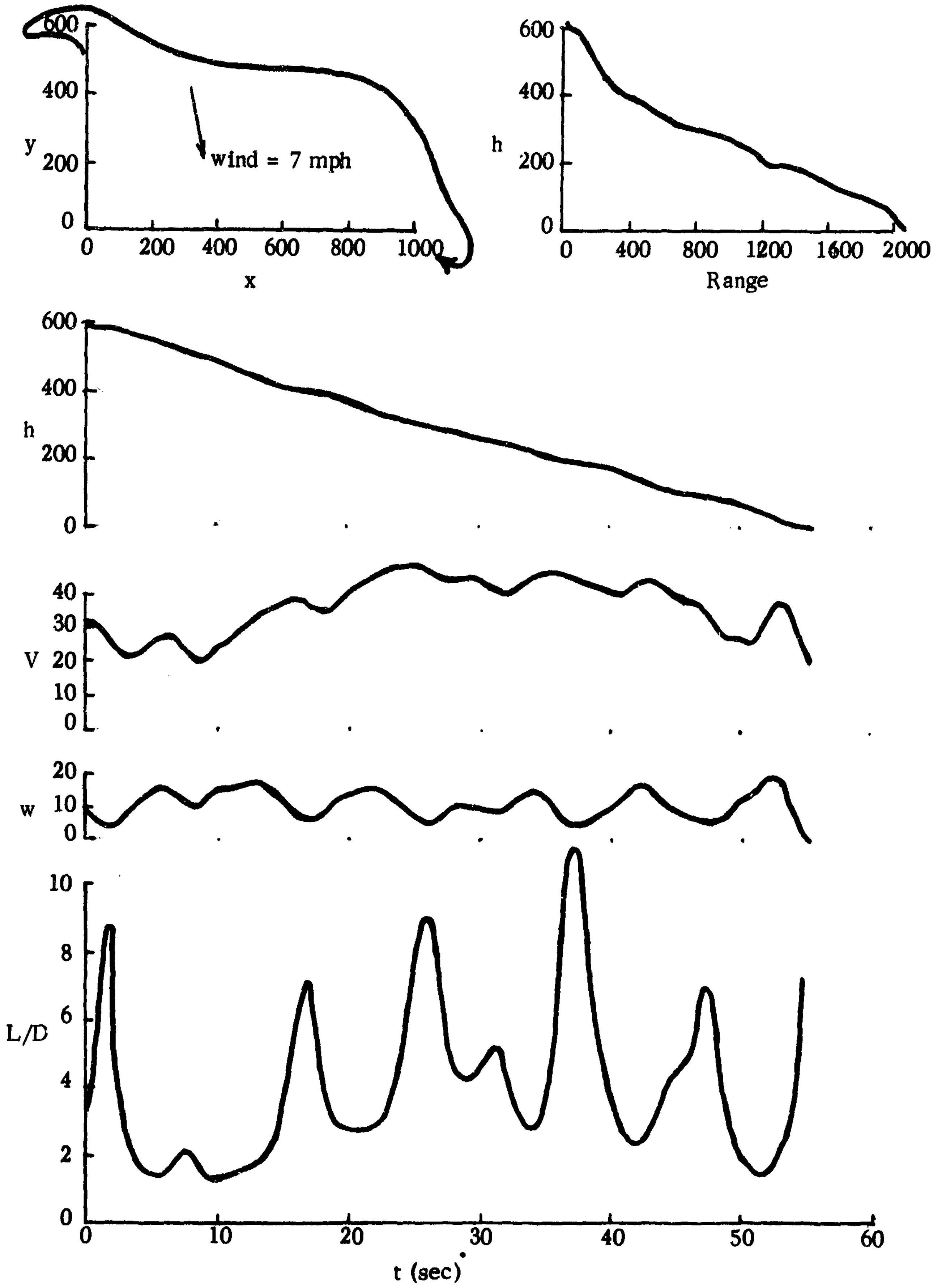

Figure 13b. Air Force Ascending Flight Data (611) University of Dayton

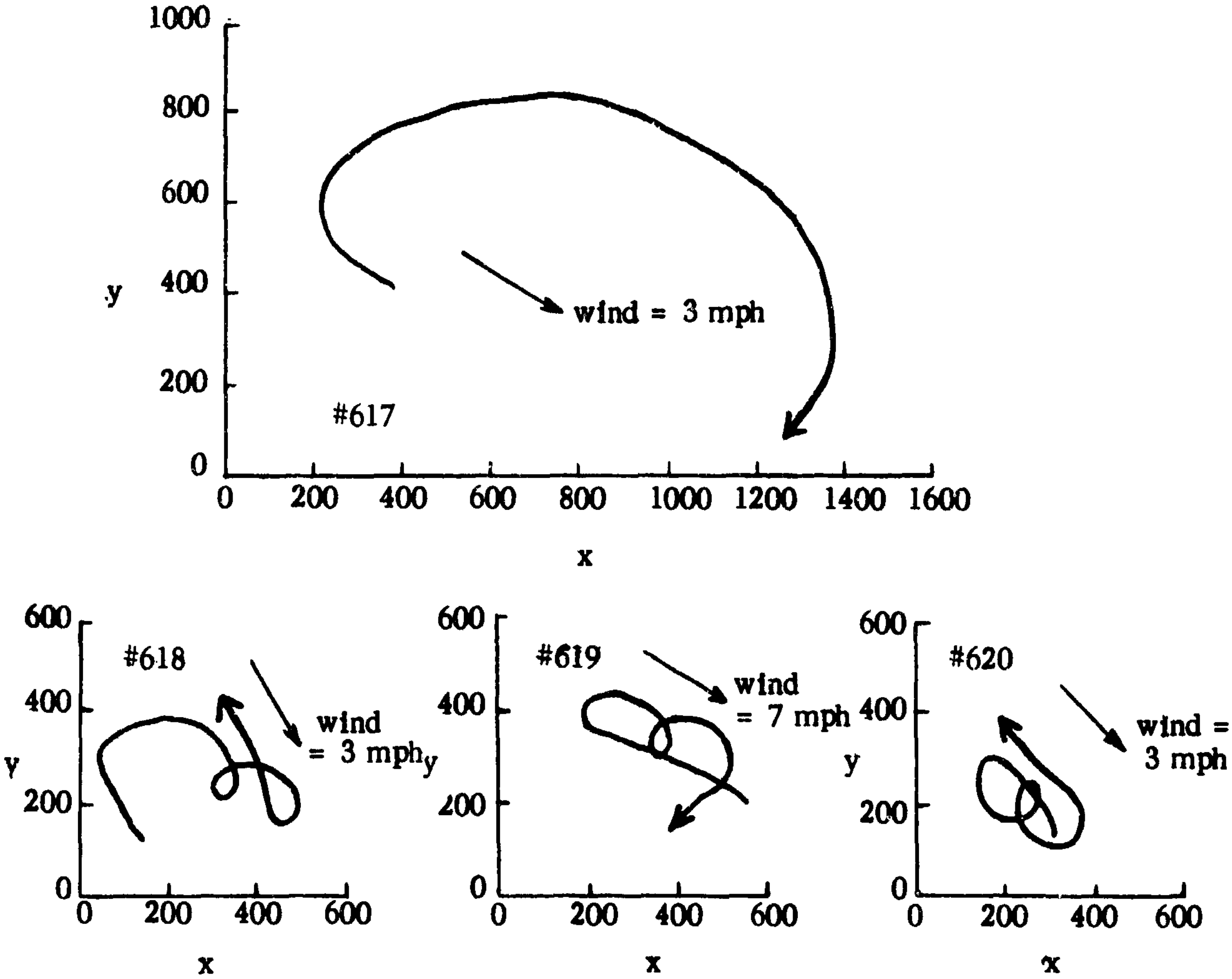

Figure 14. Parafoil Maneuvering and Turning Flights

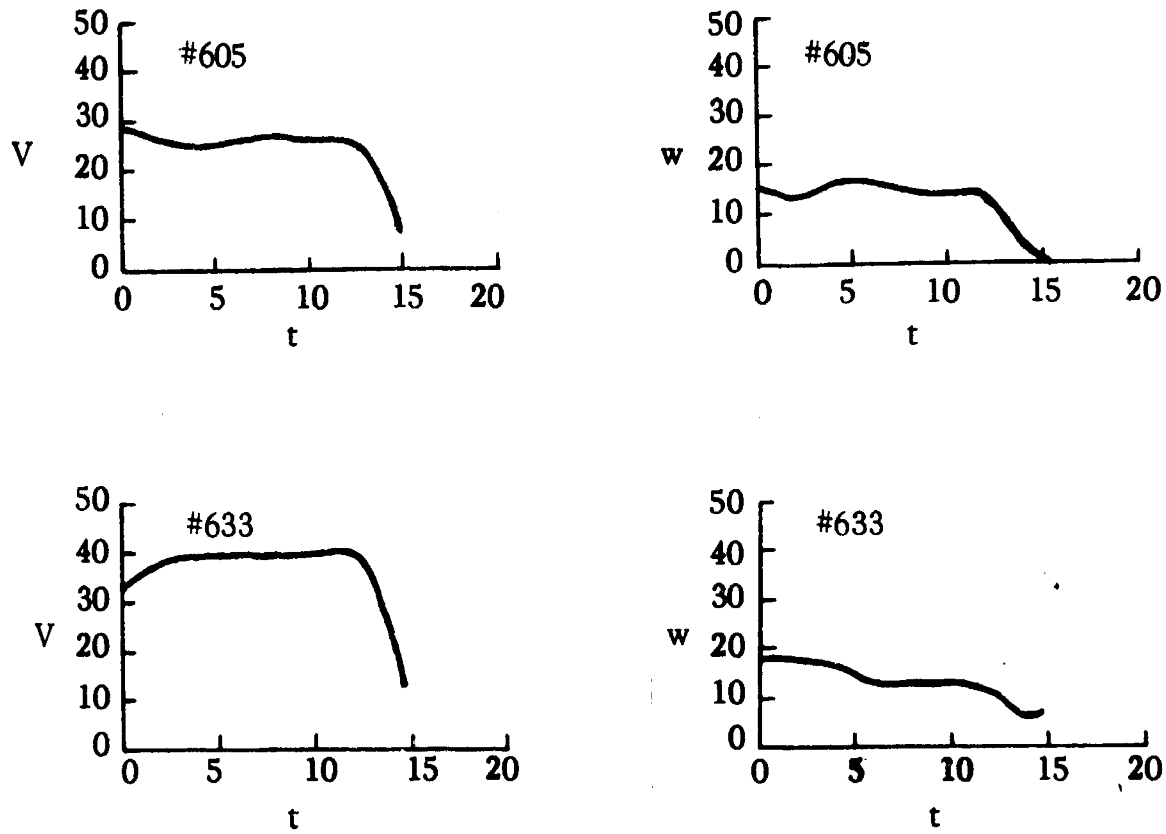

Figure 15a. Air Force Phototheodolite Data on Flare Maneuver - University of Dayton

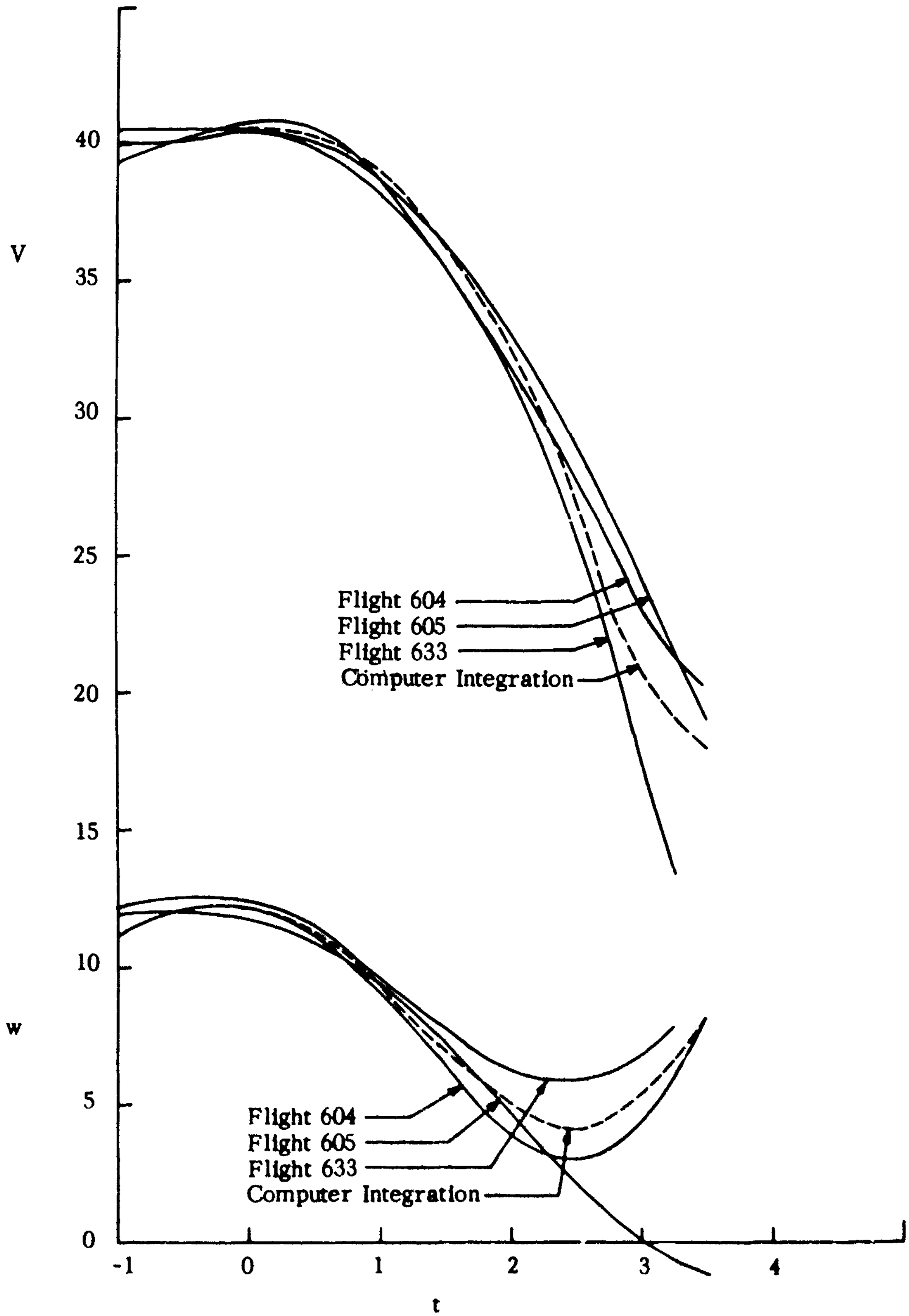

Figure 15b. Comparison of Theory and Experiment on Flare Maneuver.

TABLE II

LANDING FLARE MANEUVER COMPUTATION

Time	U Vel	W Vel	Total V	X Ft	Z Ft	CL	CD
.00	38.75	12.02	40.57	.00	.00	.477	.151
.25	38.68	11.67	40.40	9.68	2.96	.477	.151
.50	38.55	11.40	40.20	19.33	5.84	.477	.151
.75	38.33	10.16	39.65	28.95	8.53	.544	.166
1.00	37.90	9.20	39.00	38.48	10.94	.544	.166
1.25	36.65	7.72	37.46	47.80	13.04	.603	.221
1.50	35.31	7.00	36.00	56.80	14.87	.603	.221
1.75	33.72	5.52	34.17	65.43	16.41	.723	.258
2.00	32.11	5.00	32.49	73.66	17.71	.723	.258
2.25	29.47	3.77	29.71	81.35	18.77	.893	.393
2.50	27.21	4.00	27.50	88.43	19.71	.893	.393
2.75	23.04	3.86	23.36	94.68	20.64	1.143	.812
3.00	20.27	5.50	21.00	100.06	21.79	1.143	.812
3.25	17.69	6.33	18.79	104.78	23.24	1.537	1.147
3.50	16.12	8.00	18.00	108.99	25.02	1.537	1.147

X = Horizontal Distance

Z = Vertical Distance

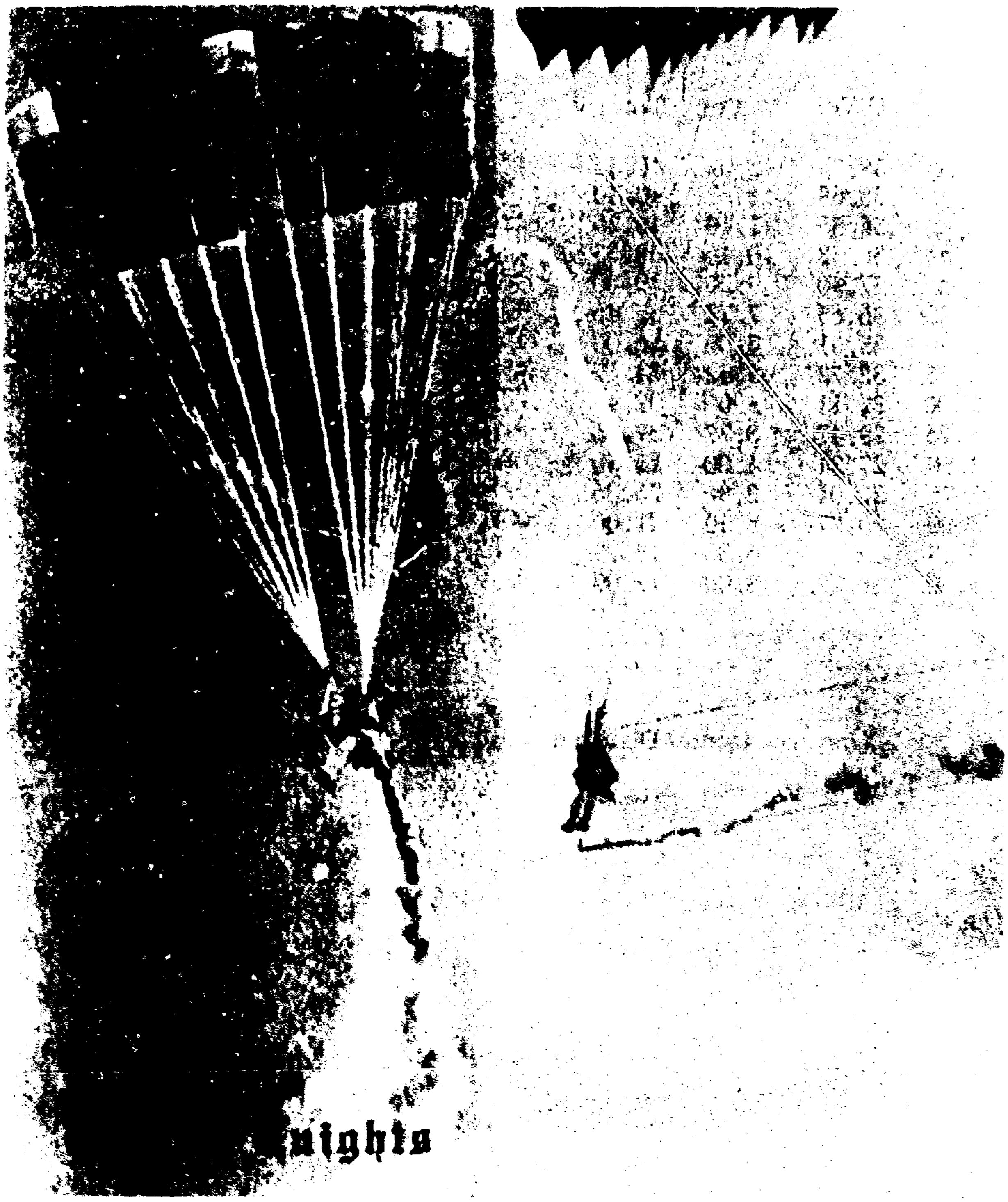

(a) (b)

Figure 16a. U.S. Army Parachute Team
16b. Air Force Jump Flight Tests

TABLE III

SUMMARY PARAFOIL FLIGHT PERFORMANCE

Ascending Flight Data

Parafoil	w	u	V	V_{mph}	L/D	W/A
ND 2.0 (200)	10.5	36	37.6	25.6	3.4	.925
ND 2.0 (242)	8.0	30	31.0	21.2	3.7	.77
ND 2.0 (360)	6.5	24	24.8	17.0	3.7	.55

Jump Flight Data

ND 2.0 (200)						
(2 chutes and bag)	11	41.0	42.5	29	3.7	1.0
(clean)	10	44.4	45.5	31	4.4	1.0
ND 2.0 (360)[8]	8.4	--	--	--	4.5*	.59
ND 2.0 (242)[8]	--	--	--	25^{+13}	5.5*	1.0

*Smoke measurements.

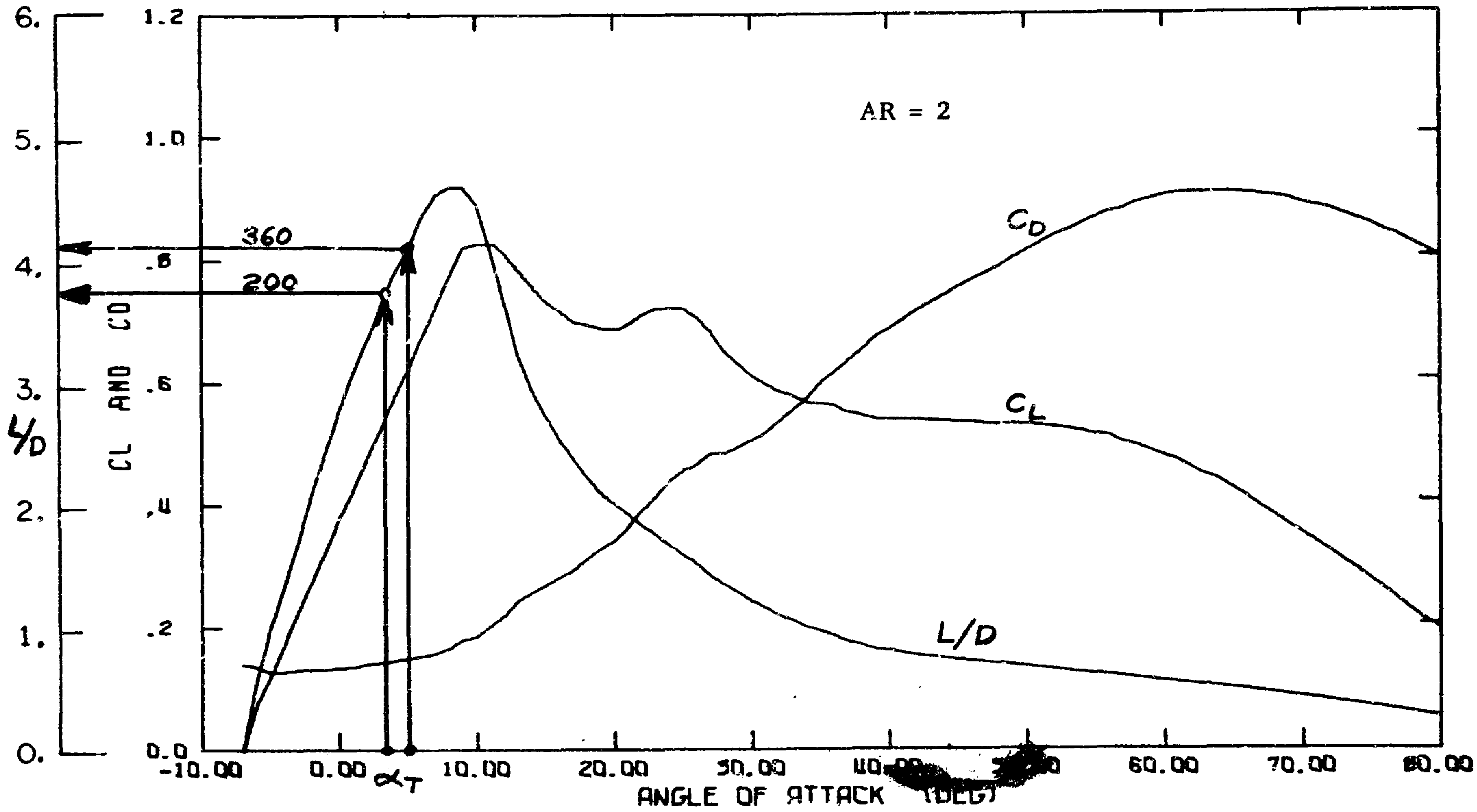

Figure 17a. Comparison of Flight Data and Prediction

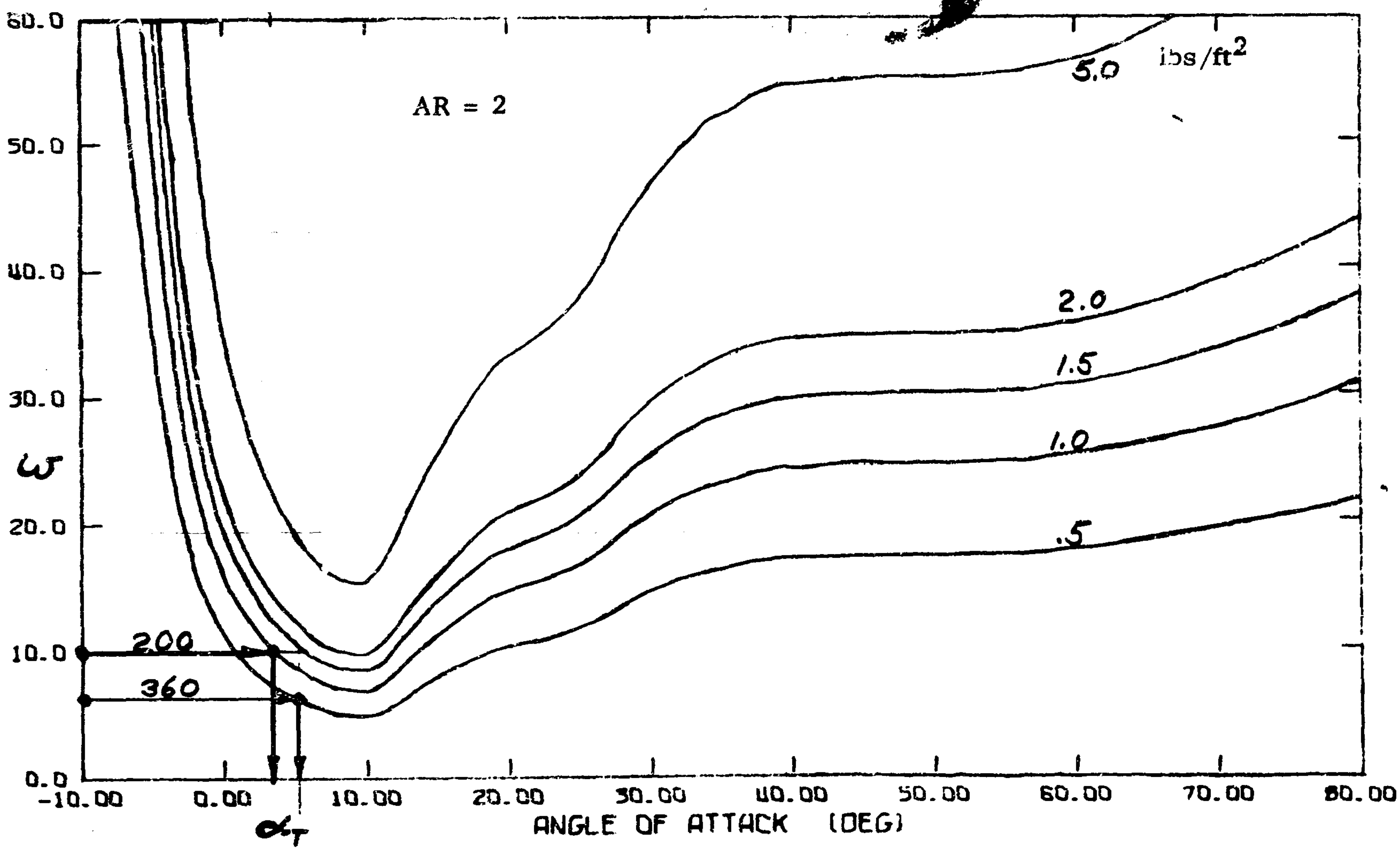

Figure 17b. Comparison of Flight Data and Prediction

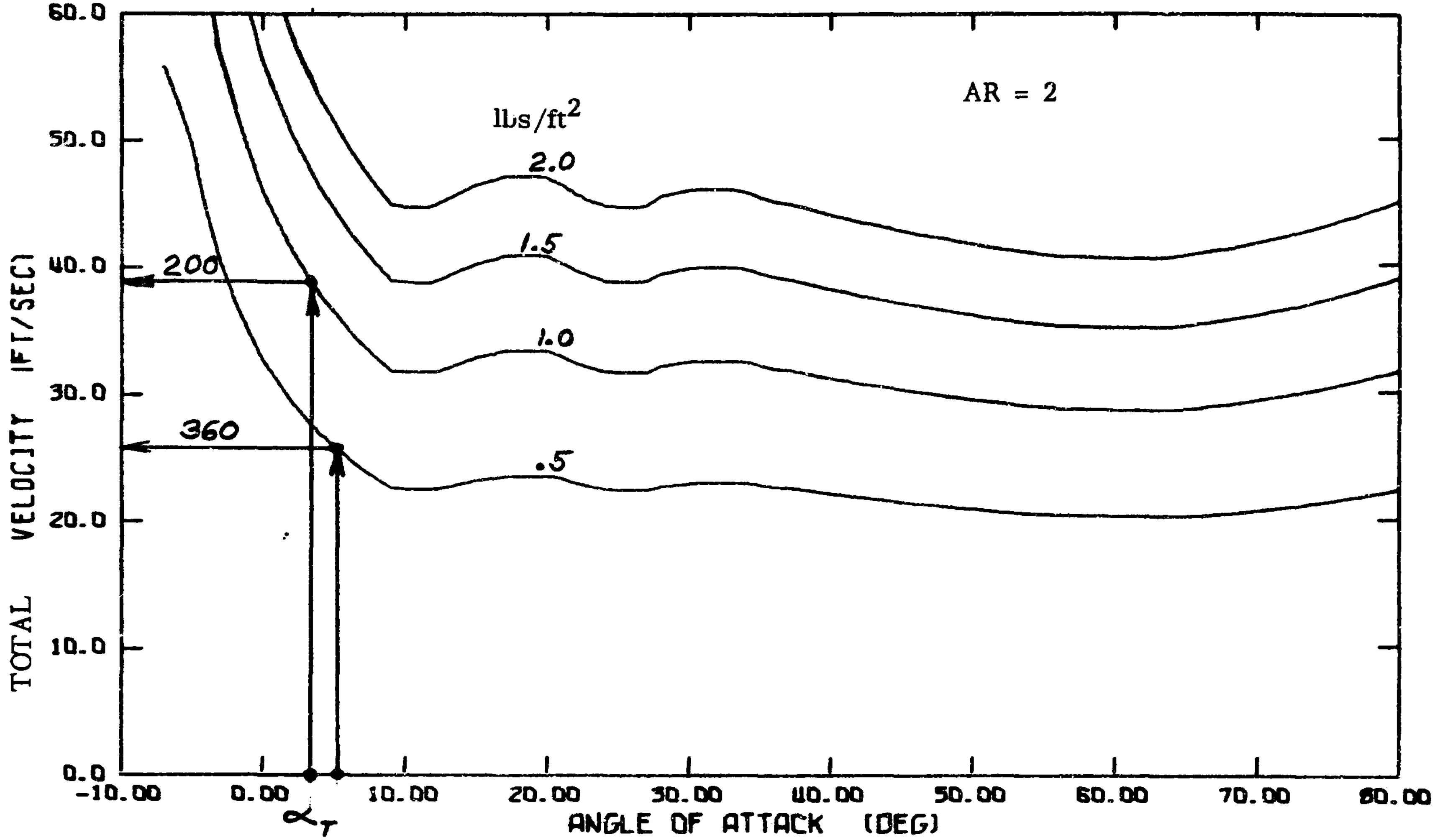

Figure 17c. Comparison of Flight Data and Prediction

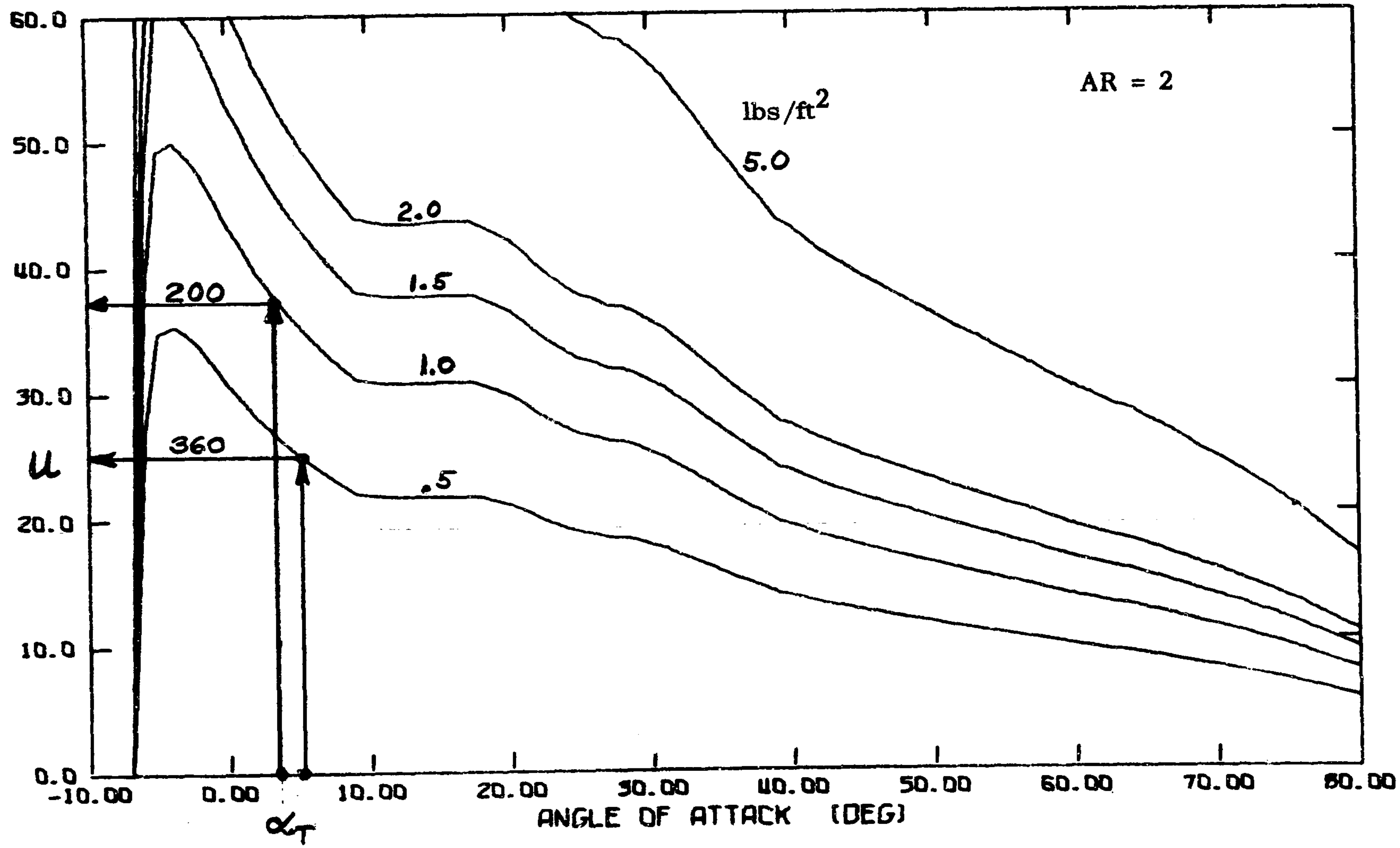

Figure 17d. Comparison of Flight Data and Prediction

APPENDIX I

COMPUTED PARAFOIL PERFORMANCE

Robert Hengstebeck*

The steady state flight performance of the Parafoil with various wing loadings ($0 < W/A \leq 10$) and at various flight trim angles ($-8^{o} \leq \alpha_T \leq +67^{o}$)** may be computed from the wind tunnel data which is now available on Parafoils of aspect ratios 1.0, 1.5, 2.0, 2.5, and 3.0. A summary of the wind tunnel lift coefficient data is provided in Figure I-1 for Parafoils of various aspect ratios.[8,11] It should be noted that the Parafoil does not exhibit the stall range of angle of attack from -8^{o} to over 75^{o}. The important lift to drag ratio plotted as a function of trim angles of attack is given in Figure I-3.[8] The corresponding wind tunnel drag coefficient data is illustrated in Figure I-2.***

Utilizing the equations of steady state motion given in the basic report, the flight performance of the various aspect ratio Parafoils is computed. Table I-1 lists the aerodynamic data used in the calculation of the performance of all the aspect ratios. The results of these computations are shown in Figure I-4 and Figure I-5 for a wing loading of 1.0. In Figure I-4 the rate of sink is plotted as a function of angle of attack for each aspect ratio, and in Figure I-5 the total velocity is plotted for each aspect ratio. In order to easily find the maximum wing loading allowable for a given rate of sink Figures I-6 through I-15 were generated. Each curve represents a constant rate of sink, and rates of sink from 2 feet per second to 50 feet per second are represented for each aspect ratio.

---

*Research Assistant.

**At the time of these computations, wind tunnel data beyond 67^{o} was not available.

***The model used in the Notre Dame wind tunnel tests had various proturbences (e.g. bolts, nuts, and thick metal flares) which were required in the construction and mounting of this semi-fabric model. The additional estimated drag coefficient due to these proturbences is $C_D \approx .023$. The standard flight Parafoil ND 2.0 (200) has line and payload drag estimated to be $C_D \approx .026$. Since these estimated additional drag coefficients are approximately the same, the wind tunnel data may be considered to represent a complete flight Parafoil with lines and payload. The line drag estimate is based on an area of 5.5 ft^2 and a drag coefficient of .6 (Fig. 18, Hoerner).[14]. The payload drag estimate is based on an area of 2.5 ft^2 and a drag coefficient of .8.

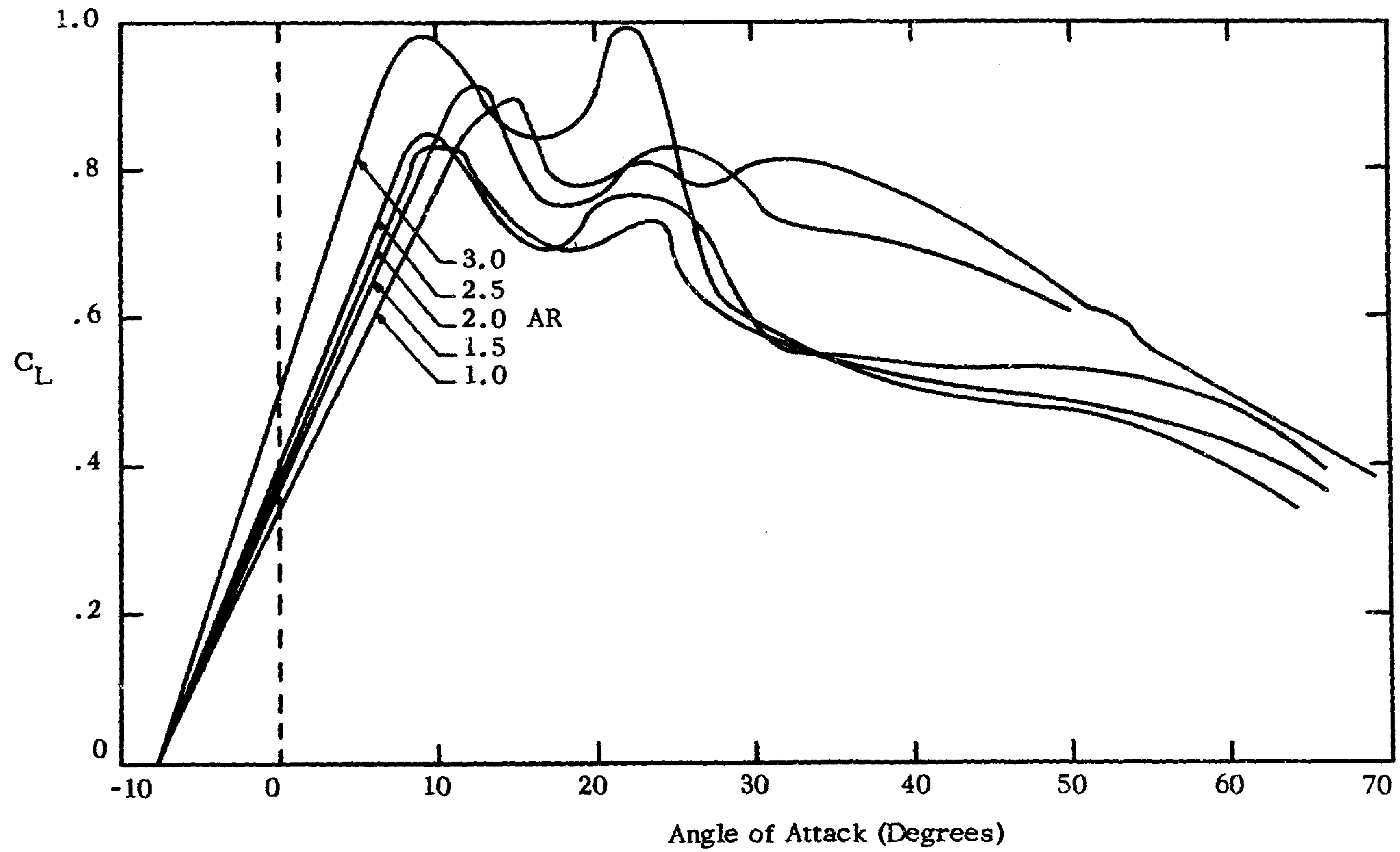

Figure I-1 Lift Coefficient Summary

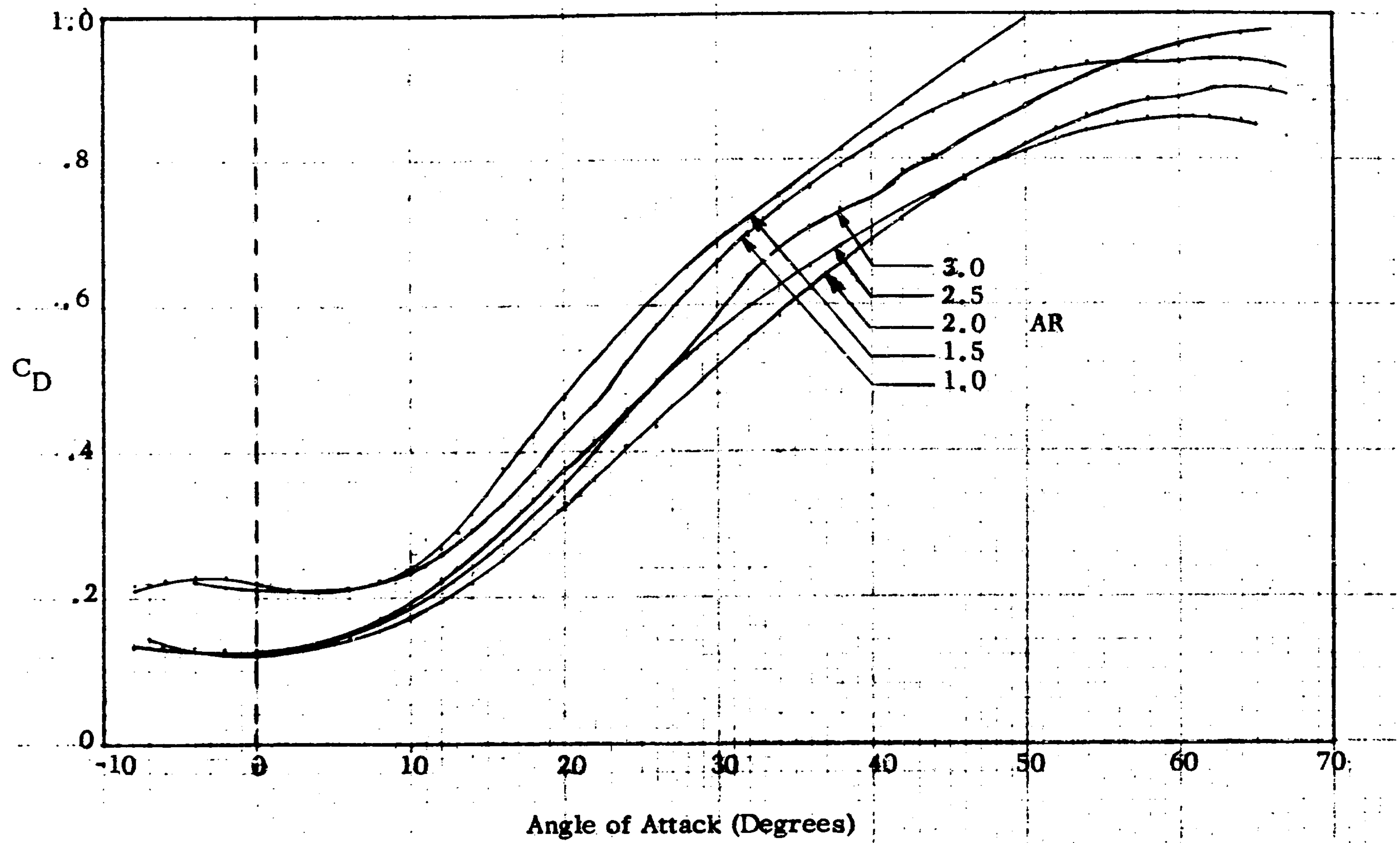

Figure I-2. Drag Coefficient Summary

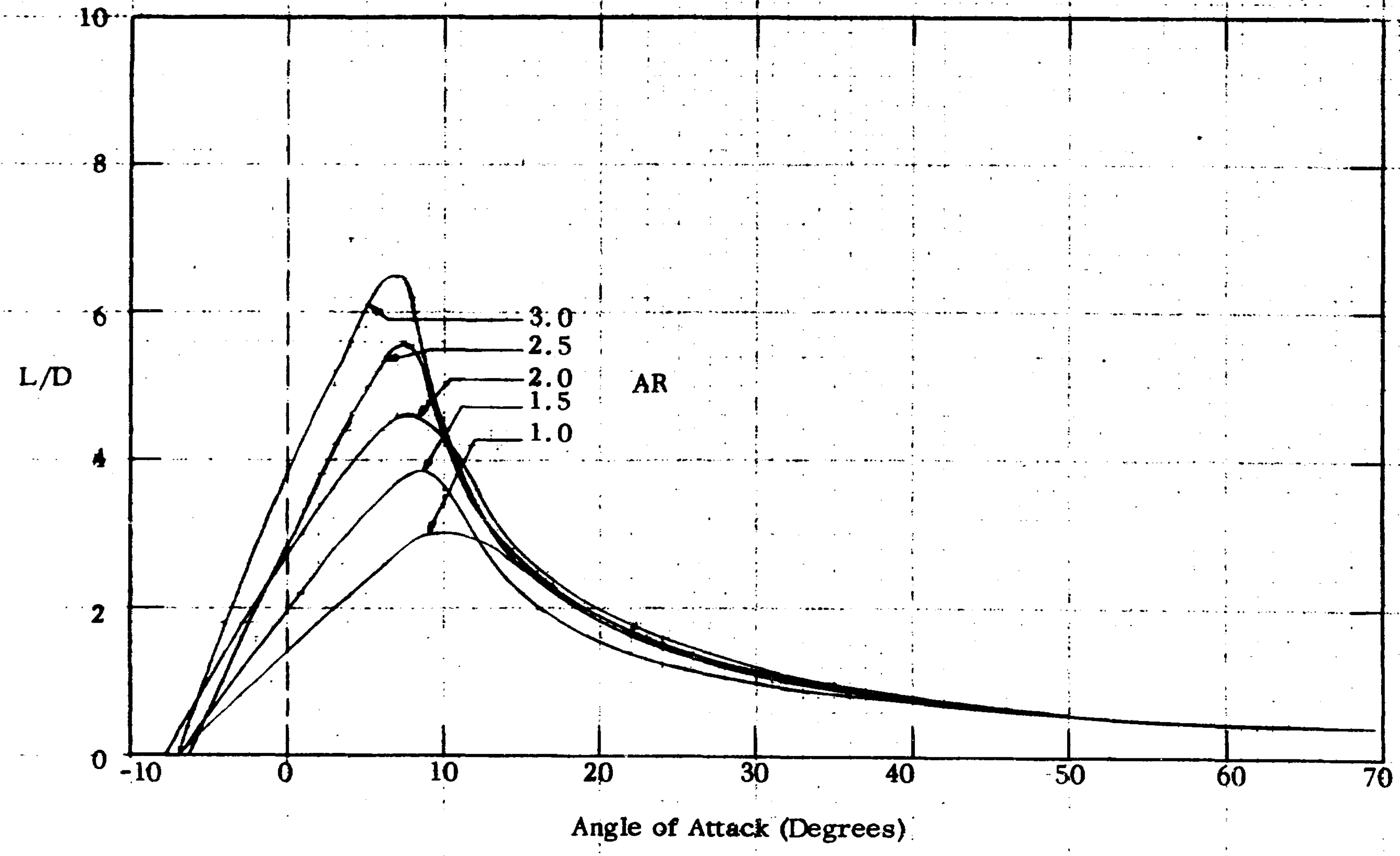

Figure I-3 L/D Summary

TABLE I-1

AERODYNAMIC DATA FOR VARIOUS ASPECT RATIO PARAFOILS

α (deg)	C_L AR 1.0	C_L AR 1.5	C_L AR 2.0	C_L AR 2.5	C_L AR 3.0	C_D AR 1.0	C_D AR 1.5	C_D AR 2.0	C_D AR 2.5	C_D AR 3.0	L/D AR 1.0	L/D AR 1.5	L/D AR 2.0	L/D AR 2.5	L/D AR 3.0
-7	.002	.037	.000		.043	.218	.223	.144		.131	.003	.223	.228		.359
-6	.037	.083	.077		.109	.221	.225	.139		.130	.230	.476	.590		.762
-5	.079	.132	.121	.099	.175	.222	.228	.137	.124	.128	.421	.708	.993	.726	1.257
-4	.126	.179	.172	.158	.235	.222	.228	.135	.124	.126	.605	.974	1.333	1.147	1.742
-3	.171	.224	.226	.213	.302	.218	.228	.134	.121	.125	.810	1.196	1.697	1.584	2.207
-2	.214	.271	.276	.264	.364	.215	.228	.131	.121	.126	1.023	1.476	2.085	2.007	2.718
-1	.260	.317	.323	.322	.429	.214	.224	.131	.123	.126	1.219	1.697	2.435	2.424	3.187
0	.299	.365	.377	.380	.503	.213	.221	.131	.124	.126	1.413	1.956	2.772	2.848	3.682
1	.345	.413	.423	.434	.562	.210	.218	.131	.126	.126	1.621	2.219	3.106	3.252	4.158
2	.388	.461	.477	.489	.623	.210	.214	.132	.130	.130	1.829	2.465	3.348	3.667	4.638
3	.430	.506	.526	.546	.687	.210	.212	.131	.133	.131	2.018	2.710	3.619	4.082	5.112
4	.473	.553	.576	.599	.744	.211	.211	.135	.140	.139	2.193	2.967	3.882	4.470	5.607
5	.514	.602	.622	.659	.811	.212	.212	.138	.146	.143	2.397	3.221	4.101	4.933	6.081
6	.559	.650	.676	.714	.876	.214	.211	.143	.153	.151	2.585	3.433	4.349	5.345	6.521
7	.601	.696	.725	.762	.927	.216	.216	.148	.161	.160	2.793	3.644	4.534	5.618	6.489
8	.642	.745	.772	.821	.964	.222	.223	.155	.167	.169	2.927	3.784	4.599	5.510	5.908
9	.690	.790	.822	.846	.977	.227	.228	.164	.178	.181	3.008	3.799	4.575	5.018	5.236
10	.730	.841	.829	.844	.972	.235	.237	.174	.189	.193	3.038	3.704	4.434	4.430	4.440
11	.779	.883	.826	.828	.946	.245	.250	.185	.201	.208	3.009	3.325	4.045	3.863	3.903
12	.816	.911	.805	.798	.917	.260	.265	.194	.214	.224	2.954	3.005	3.628	3.436	3.418
13	.853	.911	.780	.761	.890	.276	.290	.207	.228	.240	2.868	2.735	3.199	3.114	3.078
14	.874	.871	.753	.734	.866	.291	.317	.220	.245	.257	2.725	2.458	2.912	2.848	2.795
15	.869	.807	.728	.711	.850	.310	.346	.234	.261	.274	2.545	2.247	2.699	2.624	2.559
16	.849	.775	.711	.701	.844	.329	.380	.251	.275	.296	2.393	2.047	2.499	2.453	2.370
17	.819	.758	.693	.697	.845	.349	.405	.266	.294	.315	2.222	1.890	2.355	2.289	2.214

TABLE I-1 (Continued)

AERODYNAMIC DATA FOR VARIOUS ASPECT RATIO PARAFOILS

	C_L					C_D					L/D				
α (deg)	AR 1.0	AR 1.5	AR 2.0	AR 2.5	AR 3.0	AR 1.0	AR 1.5	AR 2.0	AR 2.5	AR 2.0	AR 1.0	AR 1.5	AR 2.0	AR 2.5	AR 3.0
18	.795	.757	.688	.698	.852	.373	.422	.288	.315	.338	2.057	1.752	2.207	2.156	2.091
19	.780	.757	.689	.727	.869	.395	.450	.308	.337	.354	1.935	1.627	2.092	2.020	1.958
20	.779	.762	.696	.744	.922	.423	.476	.328	.357	,377	1.843	1.538	1.990	1.915	1.845
21	.786	.778	.711	.758	.976	.436	.501	.349	.375	.393	1.744	1.462	1.901	1.803	1.743
22	.797	.802	.729	.766	.992	.465	.524	.367	.401	.415	1.639	1.392	1.813	1.708	1.664
23	.803	.822	.739	.769	.978	.498	.548	.385	.426	.435	1.584	1.335	1.734	1.619	1.590
24	.809	.830	.728	.766	.934	.523	.570	.407	.451	.454	1.541	1.274	1.645	1.534	1.518
25	.811	.830	.679	.754	.858	.550	.595	.423	.472	.472	1.471	1.228	1.561	1.451	1.444
26	.810	.826	.642	.736	.760	.574	.616	.435	.494	.494	1.398	1.170	1.494	1.368	1.364
27	.808	.816	.618	.709	.673	.599	.631	.457	.518	.517	1.339	1.129	1.402	1.286	1.277
28	.801	.804	.603	.677	.624	.620	.652	.481	.533	.539	1.279	1.097	1.331	1.214	1.196
29	.796	.789	.591	.621	.605	.644	.668	.499	.549	.566	1.218	1.058	1.264	1.148	1.107
30	.787	.765	.582	.592	.592	.660	.686	.520	.565	.586	1.168	1.021	1.194	1.091	1.005
31	.776	.740	.573	.575	.580	.676	.703	.537	.582	.615	1.118	.982	1.104	1.043	.930
32	.770	.726	.563	.557	.569	.696	.719	.559	.598	.642	1.072	.955	1.047	1.003	.887
33	.758	.719	.557	.547	.560	.714	.735	.575	.612	.658	1.037	.916	1.004	.961	.859
34	.747	.718	.552	.548	.551	.731	.752	.587	.626	.675	.981	.892	.959	.933	.824
35	.733	.713	.547	.530	.543	.749	.768	.607	.638	.695	.942	.863	.914	.891	.807
36	.728	.713	.544	.531	.535	.762	.783	.624	.652	.707	.905	.832	.880	.860	.780
37	.711	.708	.541	.523	.530	.774	.799	.641	.665	.717	.879	.809	.850	.828	.732
38	.698	.703	.540	.515	.526	.790	.816	.658	.680	.731	.838	.785	.825	.787	.756
39	.683	.697	.535	.510	.520	.805	.829	.671	.694	.758	.816	.760	.791	.768	.738
40	.671	.690	.535	.505	.516	.820	.847	.688	.704	.755	.781	.739	.770	.738	.731
41	.656	.685	.534	.498	.512	.833	.863	.702	.719	.767	.747	.716	.748	.711	.715
42	.641	.677	.534	.493	.508	.842	.876	.719	.732	.783	.731	.696	.729	.688	.694

TABLE I-1 (Continued)

AERODYNAMIC DATA FOR VARIOUS ASPECT RATIO PARAFOILS

α	C_L					C_D					L/D				
(deg)	AR 1.0	AR 1.5	AR 2.0	AR 2.5	AR 3.0	AR 1.0	AR 1.5	AR 2.0	AR 2.5	AR 3.0	AR 1.0	AR 1.5	AR 2.0	AR 2.5	AR 3.0
43	.627	.669	.531	.489	.506	.855	.893	.732	.744	.792	.702	.681	.724	.662	.679
44	.611	.662	.531	.485	.503	.867	.908	.745	.753	.805	.676	.662	.705	.643	.657
45	.598	.653	.530	.481	.500	.878	.922	.762	.763	.815	.660	.645	.692	.624	.654
46	.594	.644	.530	.480	.498	.889	.936	.774	.775	.826	.630	.625	.681	.611	.631
47	.572	.635	.528	.479	.494	.894	.950	.788	.784	.841	.616	.604	.662	.594	.627
48	.557	.625	.527	.476	.491	.903	.965	.800	.795	.851	.586	.594	.641	.577	.609
49	.544	.616	.527	.476	.493	.911	.978	.812	.804	.861	.583	.577	.625	.565	.588
50	.533	.604	.527	.473	.483	.915	.994	.822	.812	.873	.562	.561	.621	.548	.585
51	.517		.526	.468	.479	.920		.833	.820	.885	.541		.599	.537	.568
52	.506		.523	.463	.475	.924		.842	.828	.894	.523		.593	.525	.548
53	.497		.518	.456	.470	.929		.851	.833	.902	.513		.578	.516	.528
54	.481		.518	.451	.467	.934		.860	.840	.915	.500		.571	.497	.526
55	.471		.513	.443	.462	.934		.864	.846	.921	.488		.558	.486	.505
56	.457		.507	.434	.454	.935		.872	.850	.931	.482		.556	.472	.486
57	.444		.502	.426	.448	.935		.877	.854	.936	.462		.548	.464	.482
58	.433		.496	.417	.442	.934		.884	.856	.945	.453		.531	.455	.462
59	.423		.486	.405	.436	.937		.888	.858	.951	.441		.530	.438	.441
60	.409		.478	.393	.428	.936		.884	.858	.957	.431		.519	.422	.430
61	.397		.467	.380	.418	.939		.893	.859	.962	.424		.512	.421	.412
62	.386		.457	.370	.409	.939		.894	.858	.966	.412		.500	.415	.395
63	.374		.443	.357	.399	.937		.897	.857	.970	.398		.485	.412	.376
64	.363		.428	.341	.390	.937		.897	.855	.972	.396		.474	.402	.357
65	.351		.409	.327	.377	.935		.895	.851	.975	.384		.465	.391	.336
66	.338		.387		.361	.932		.893		.978	.371		.451		.319
67	.328		.356		.348	.931		.890		.978	.360		.428		.315

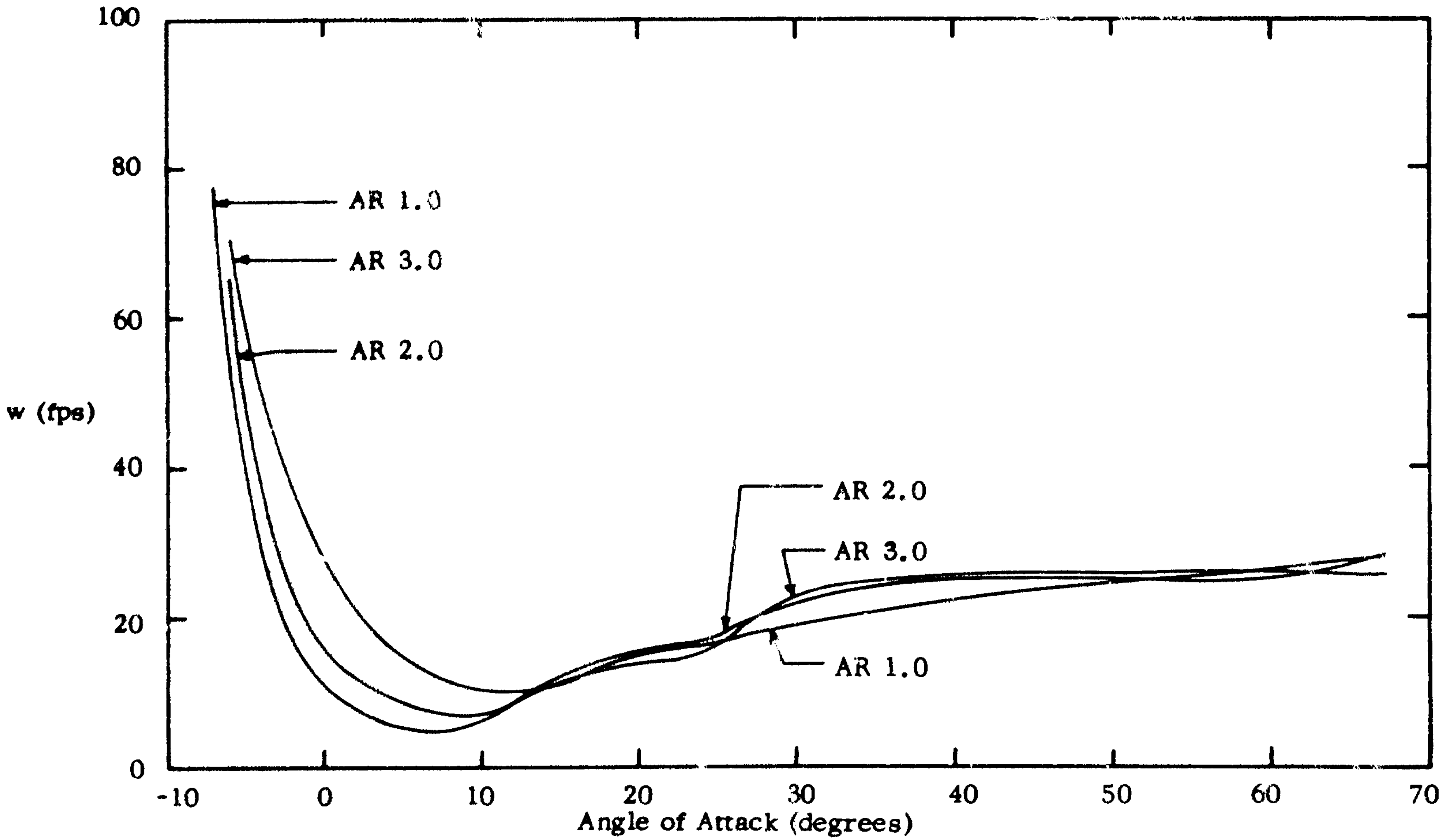

Figure I-4a. Rate of Sink of Various Aspect Ratio Parafoils (W/A= 1.0)

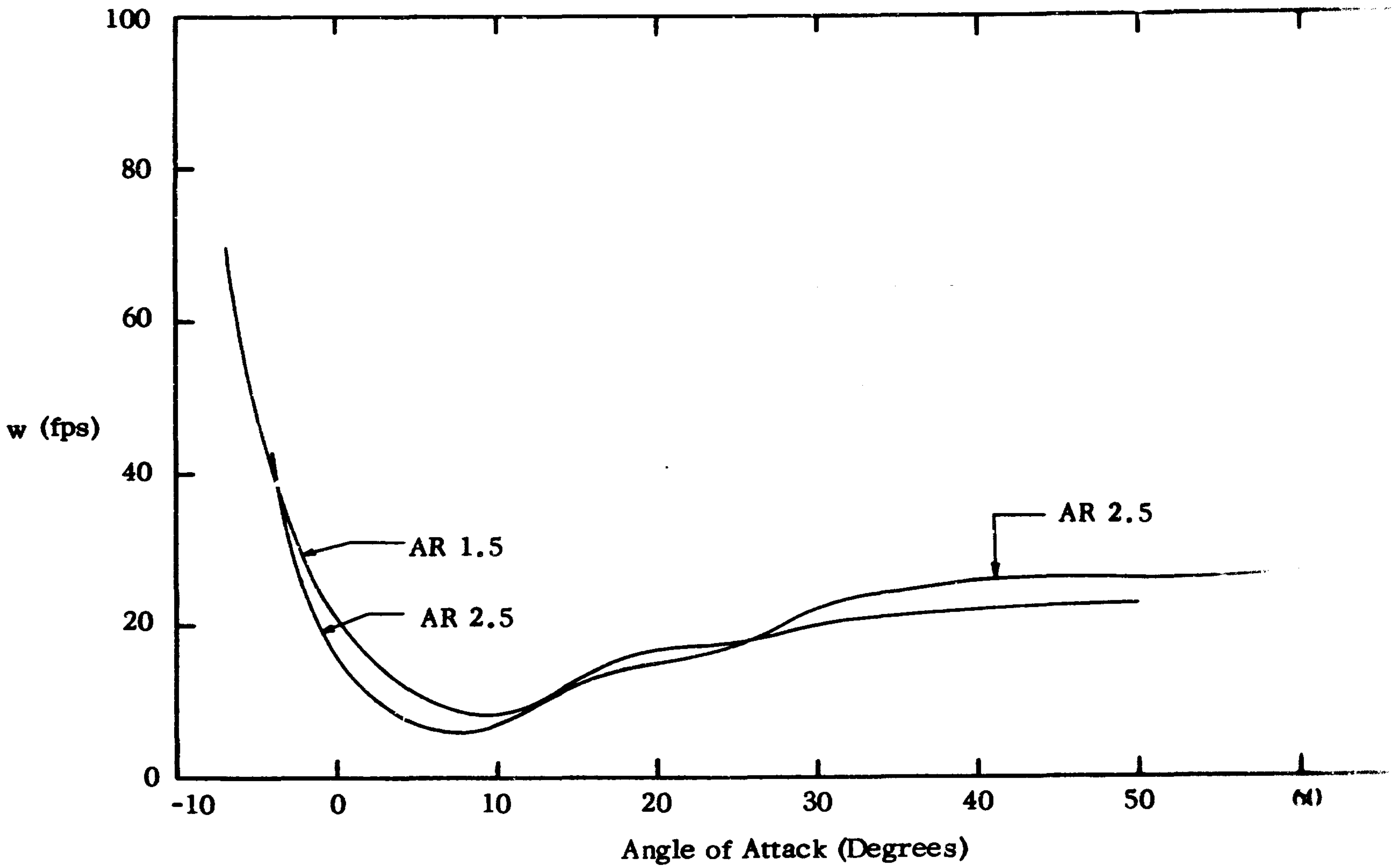

Figure I-4b. Rate of Sink of Various Aspect Ratio Parafoils (W/A=1.0)

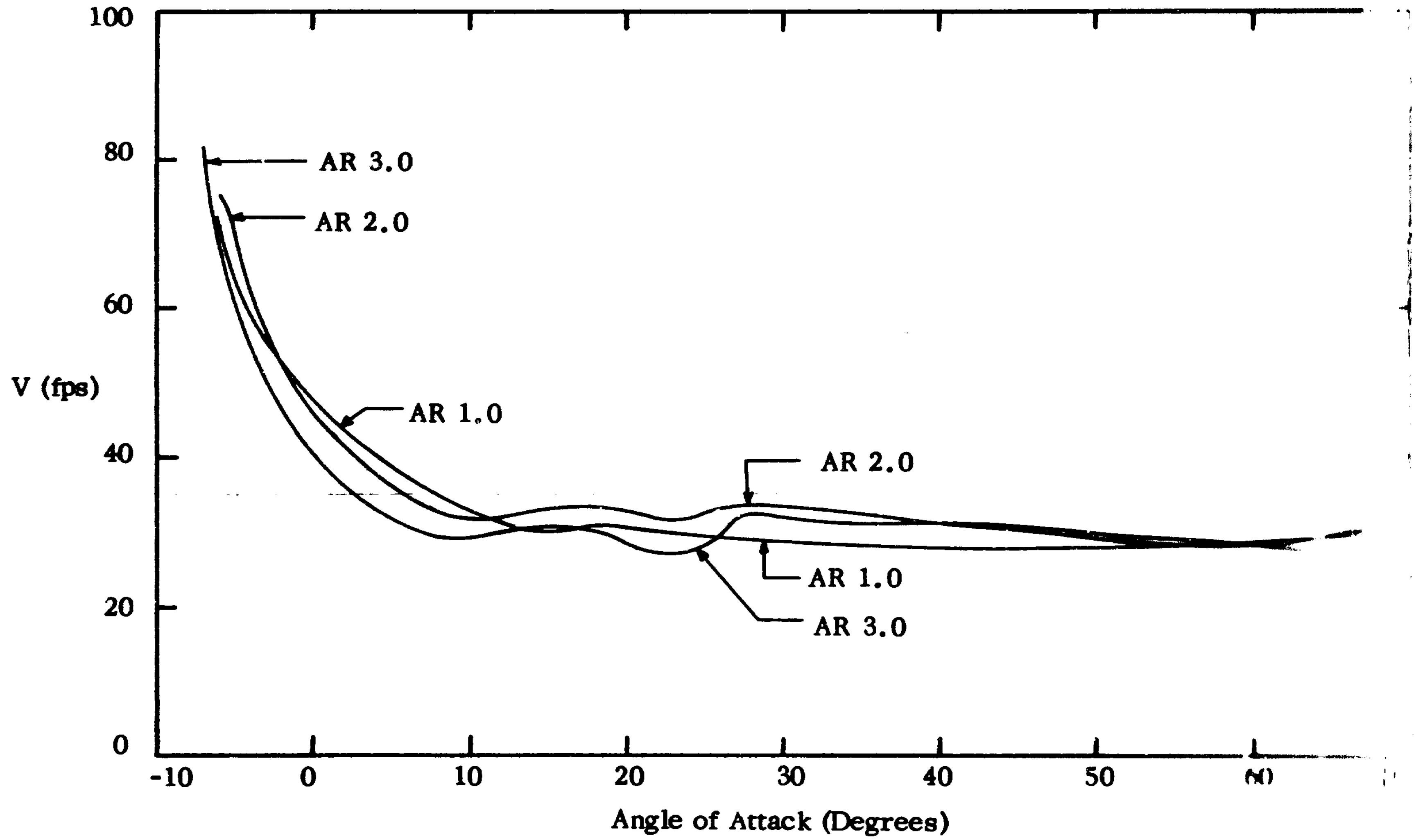

Figure I-5a. Flight Velocity of Various Aspect Ratio Parafoils (W/A=1.0)

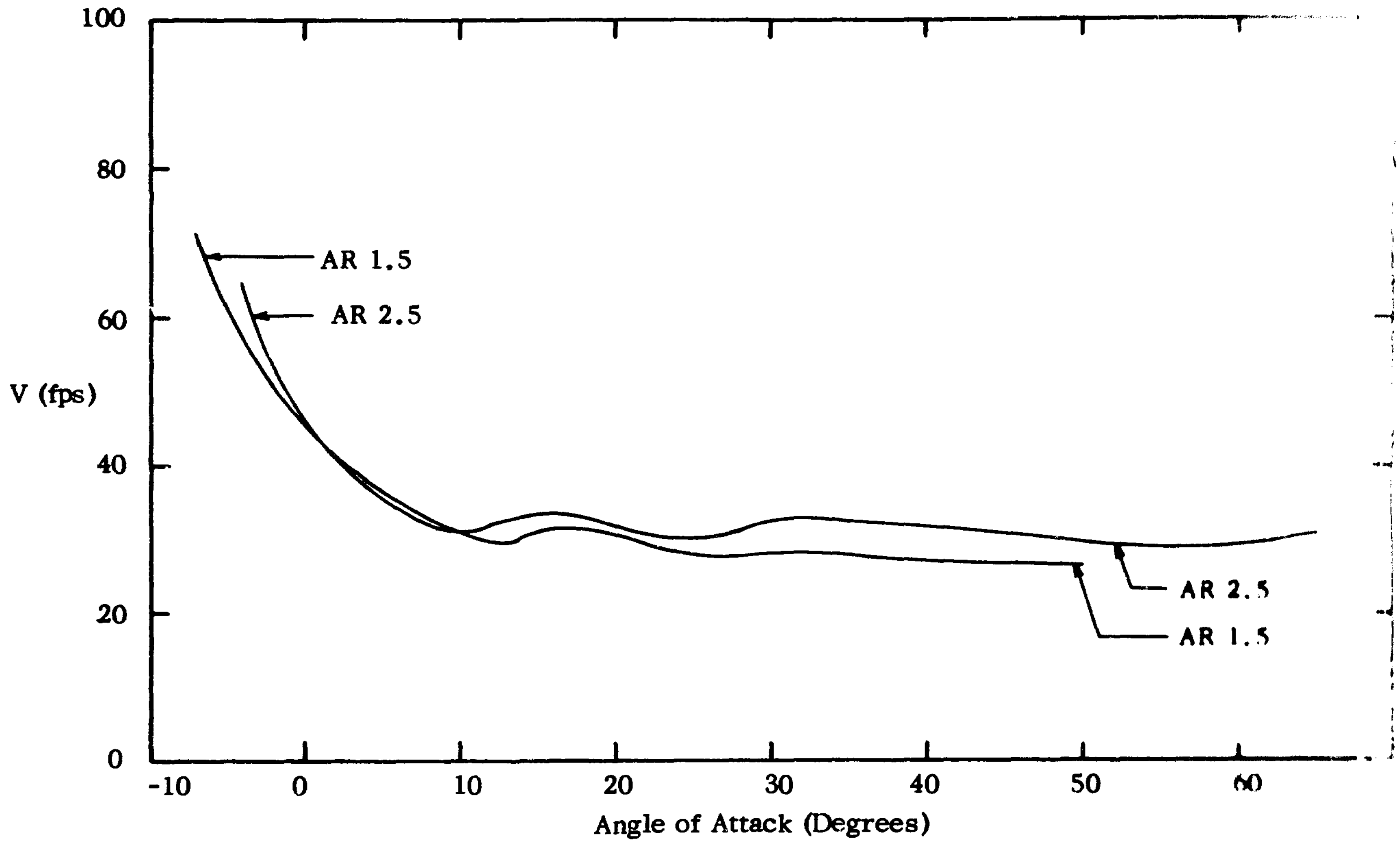

Figure I-5b. Flight Velocity of Various Aspect Ratio Parafoils (W/A=1.0)

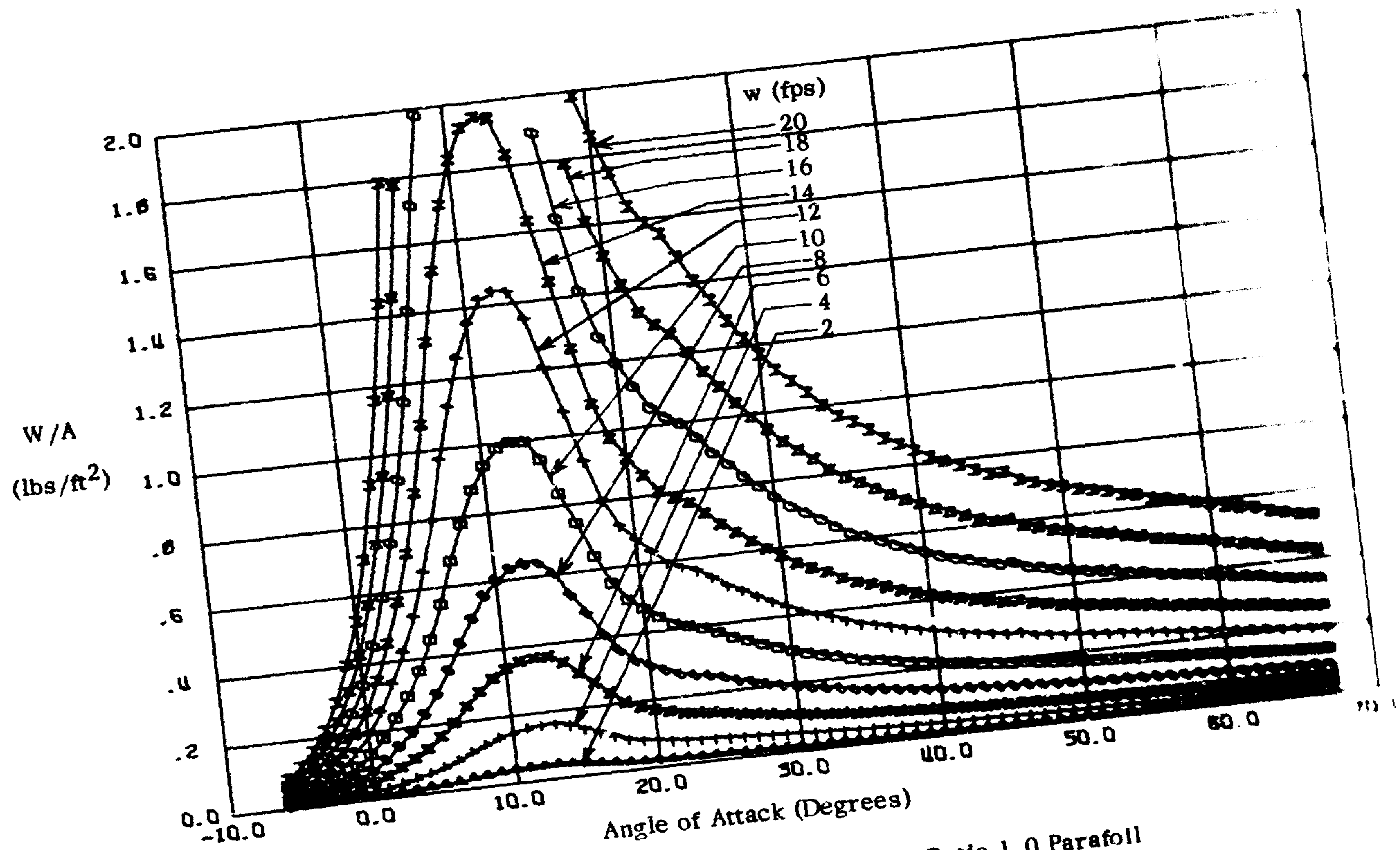

Figure I-6. Constant Rate of Sink Curves for Aspect Ratio 1.0 Parafoil

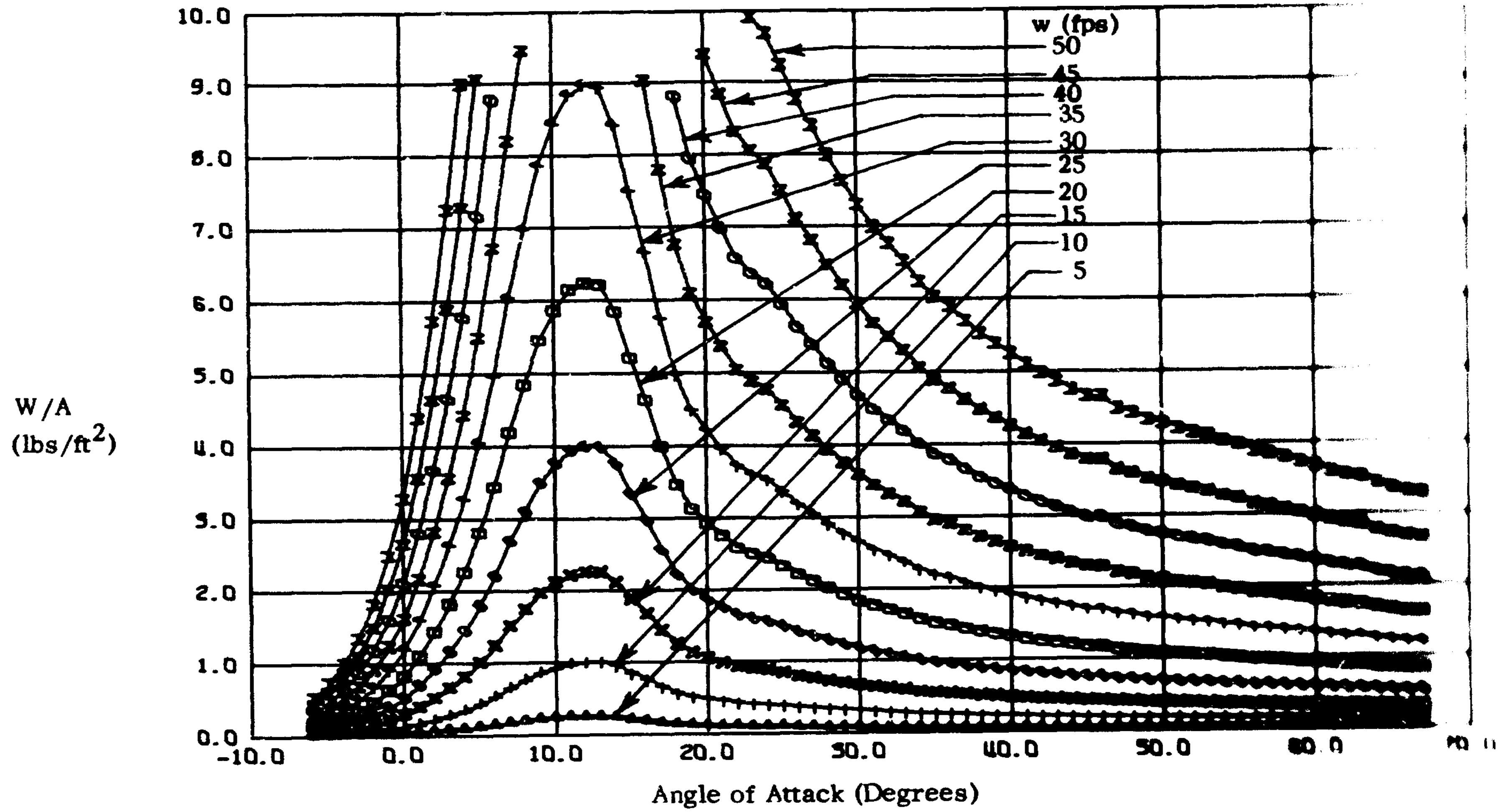

Figure I-7. Constant Rate of Sink Curves for Aspect Ratio 1.0 Parafoil

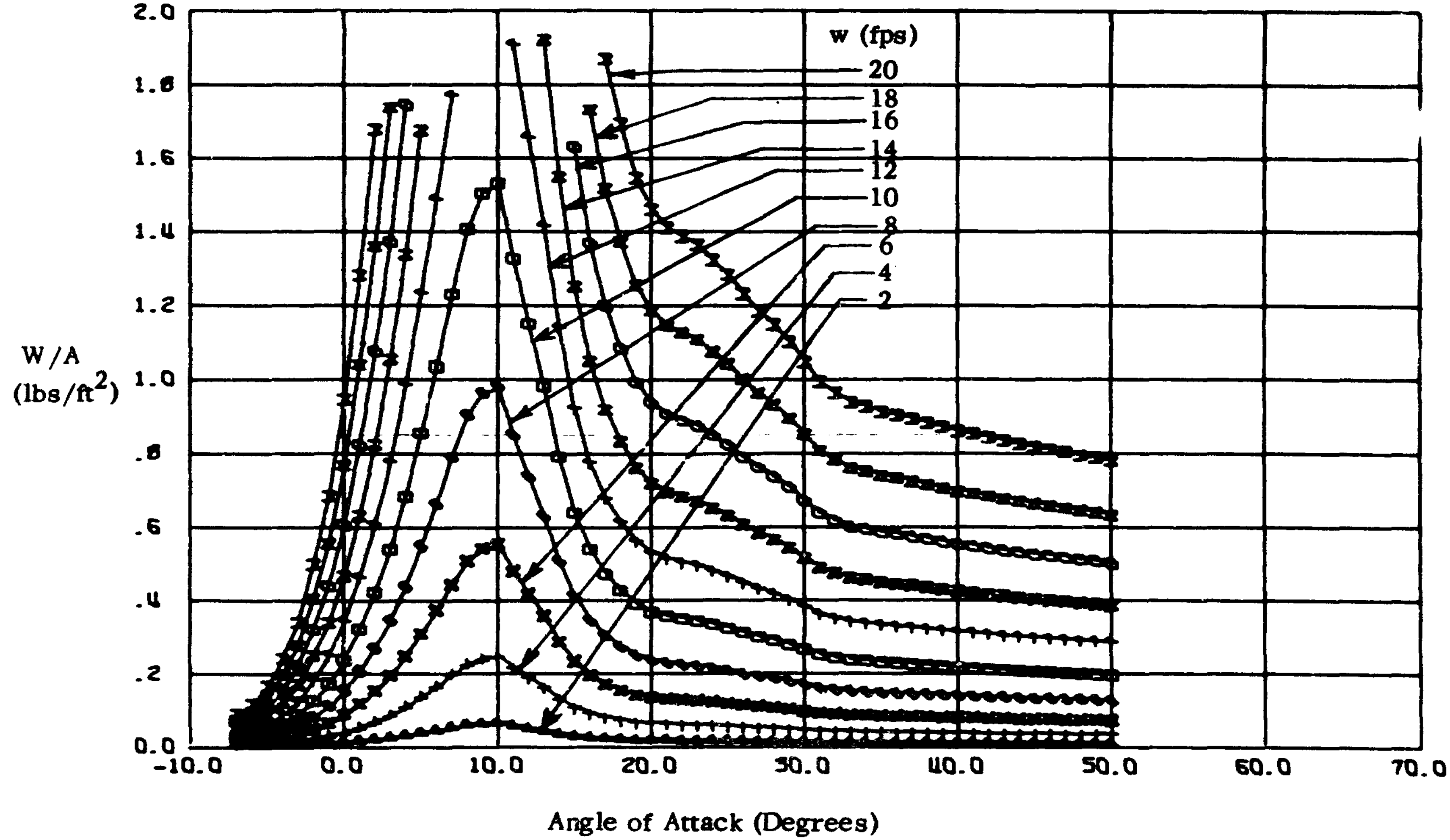

Figure I-8 . Constant Rate of Sink Curves for Aspect Ratio 1.5 Parafoil

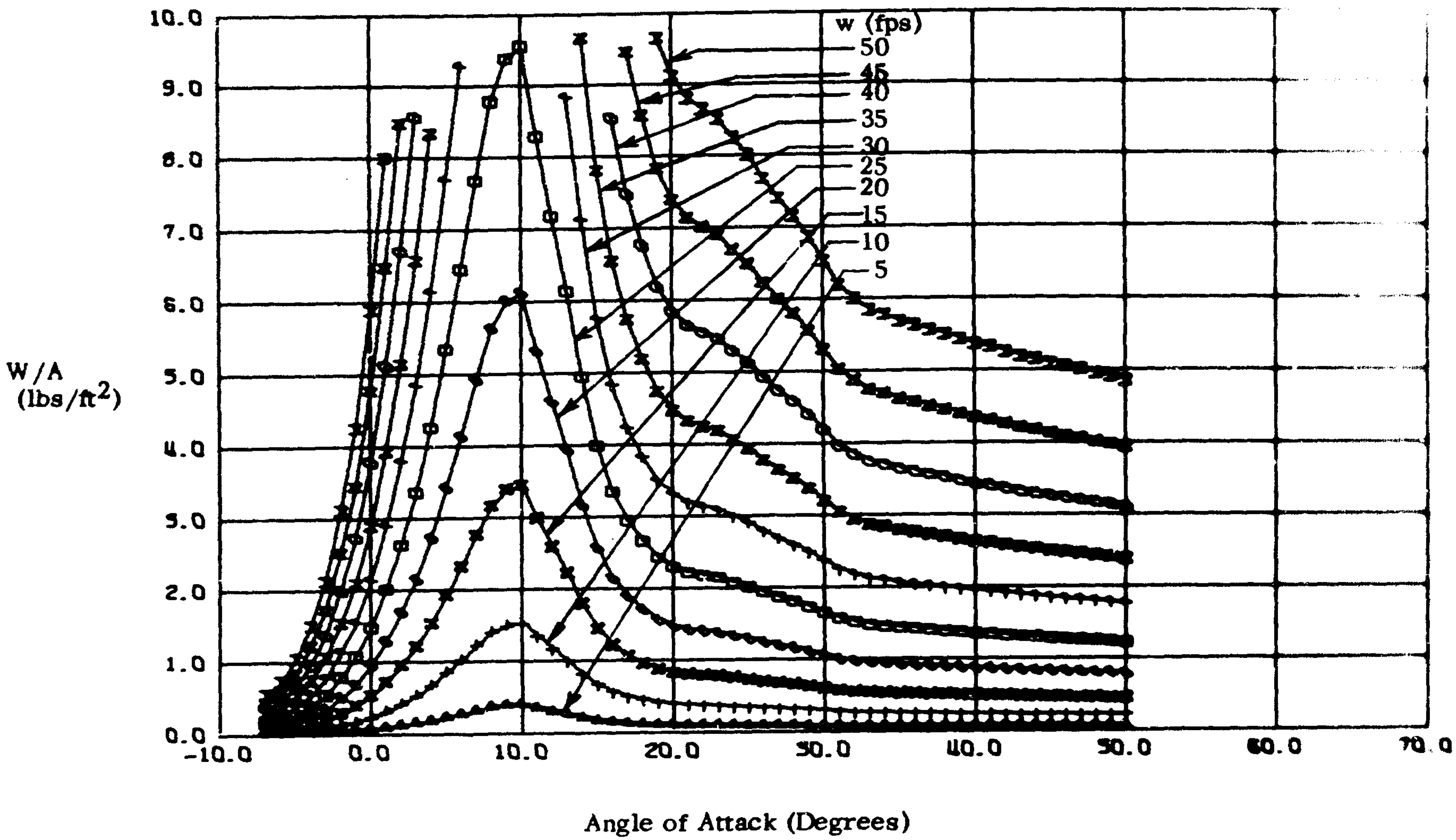

Figure I-9.. Constant Rate of Sink Curves for Aspect Ratio 1.5 Parafoil

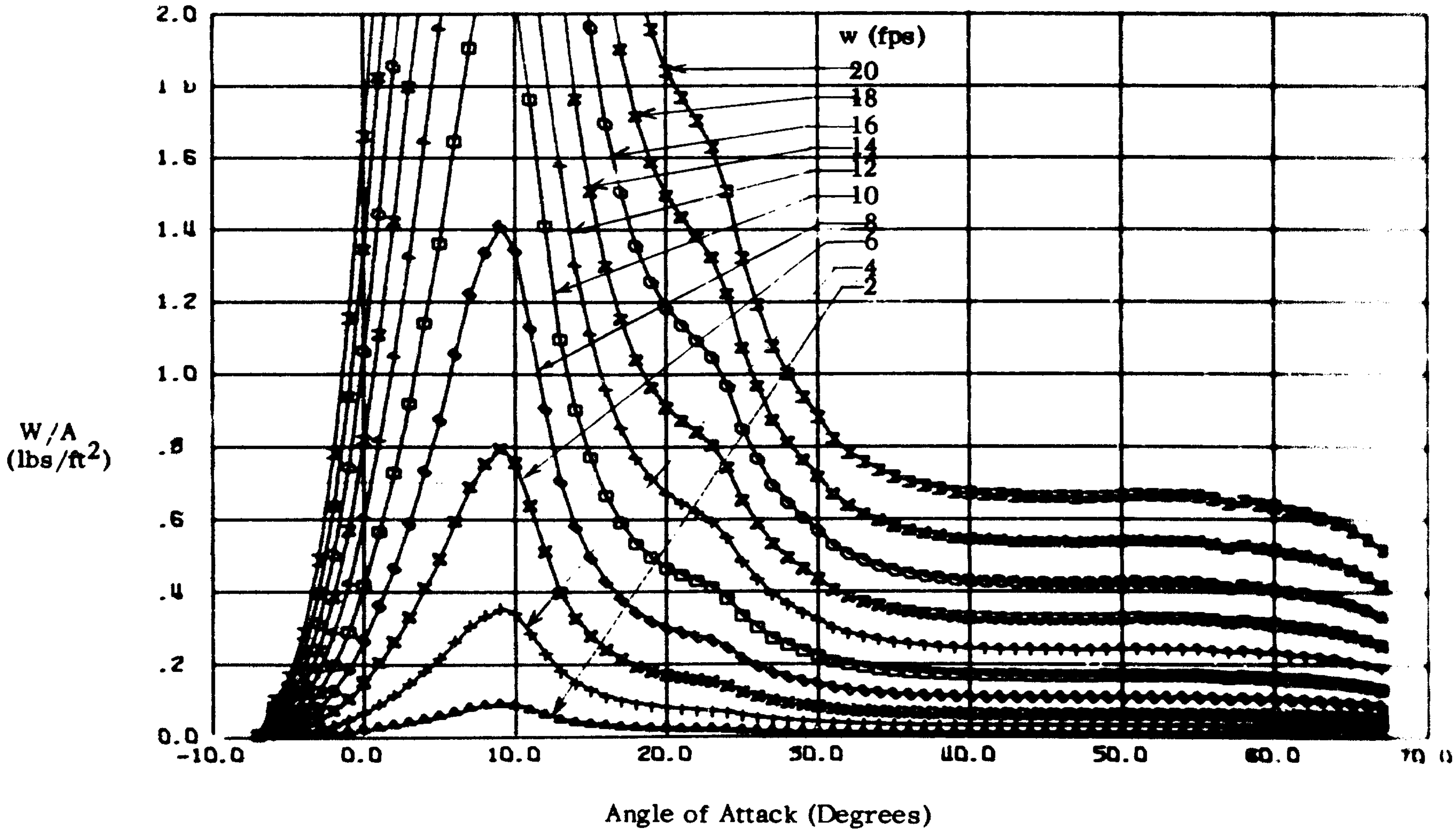

Figure I-10. Constant Rate of Sink Curves for Aspect Ratio 2.0 Parafoil

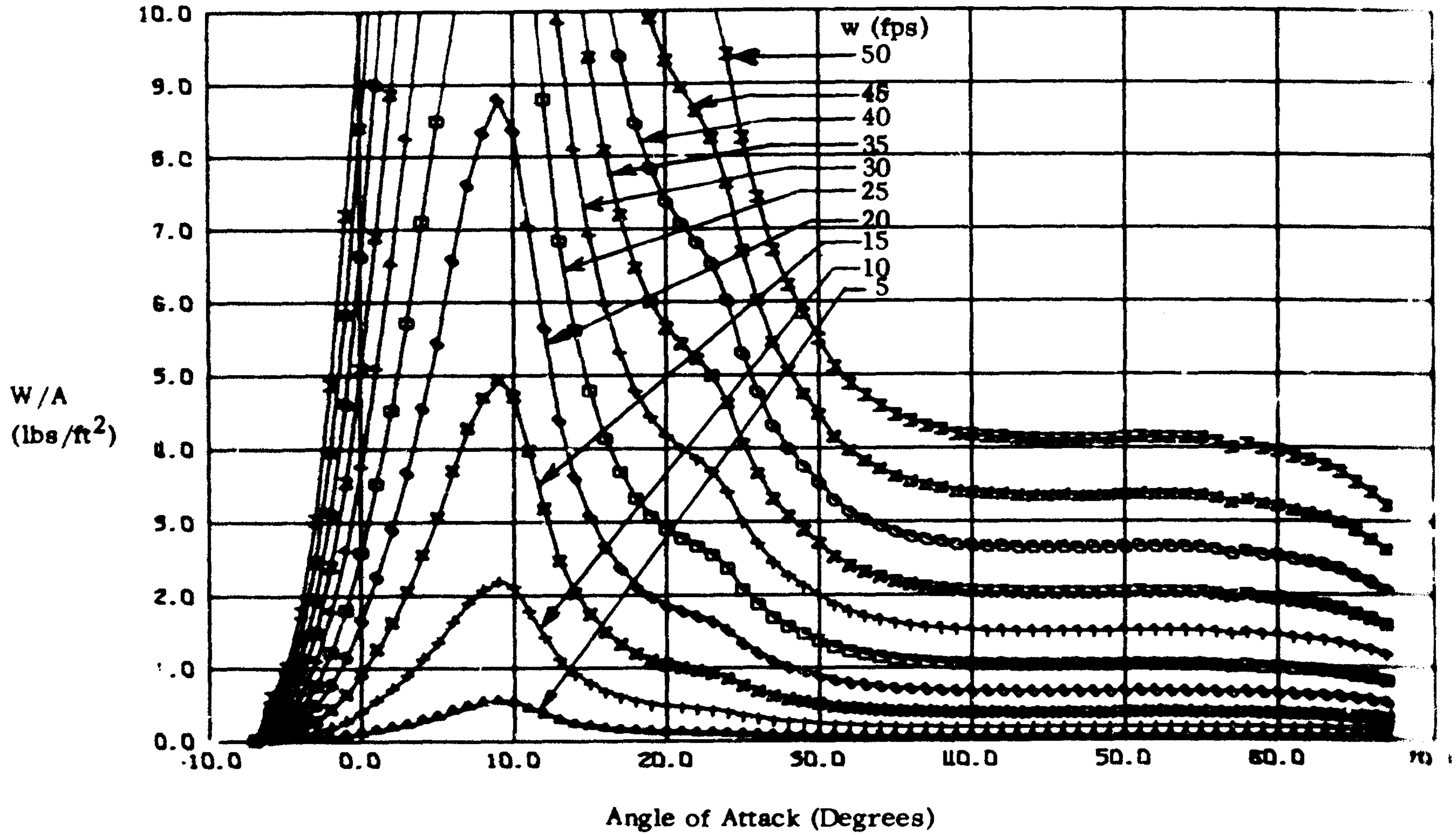

Figure I-11 Constant Rate of Sink Curves for Aspect Ratio 2.0 Parafoil

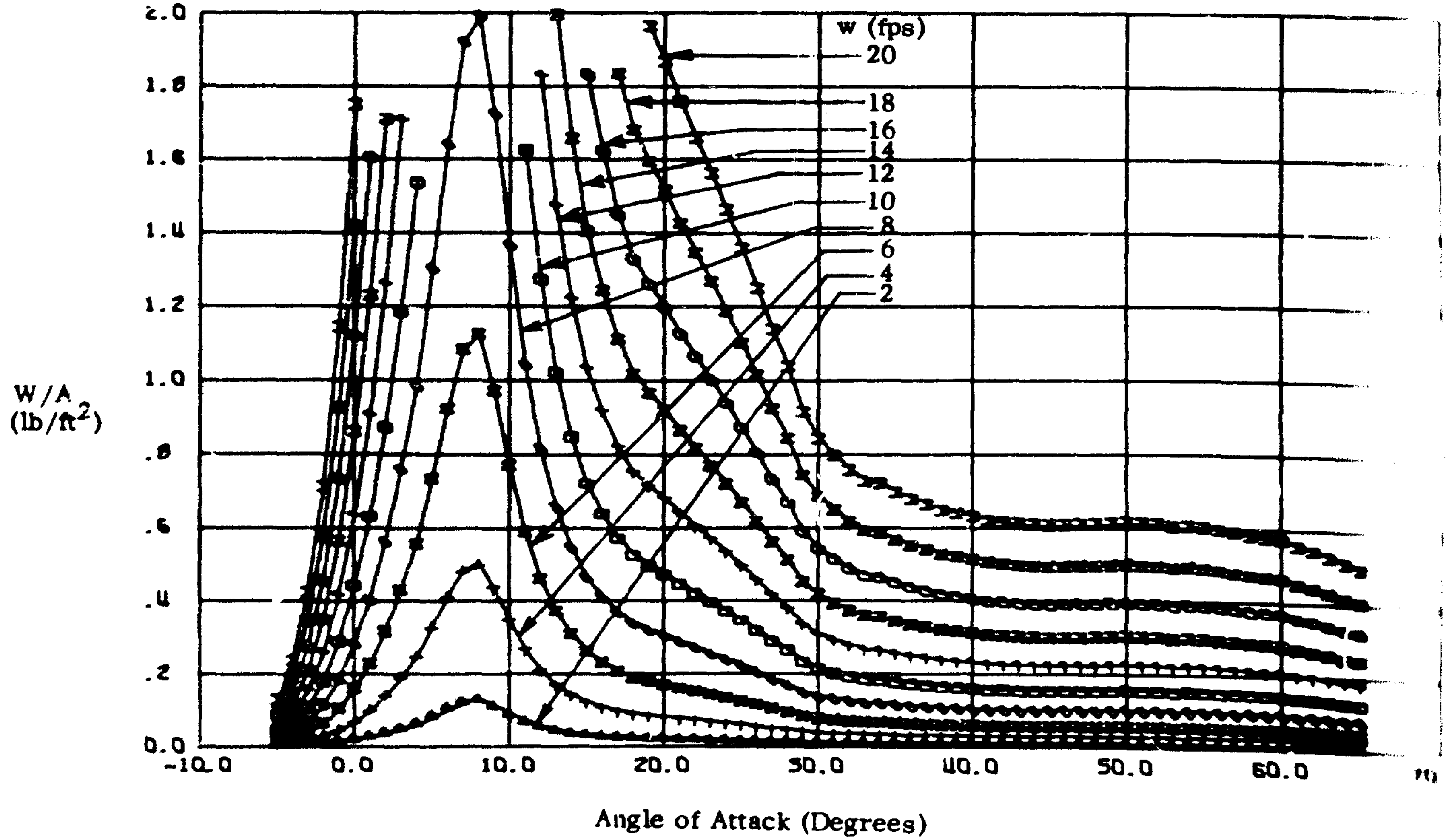

Figure I-12 Constant Rate of Sink Curves for Aspect Ratio 2.5 Parafoil

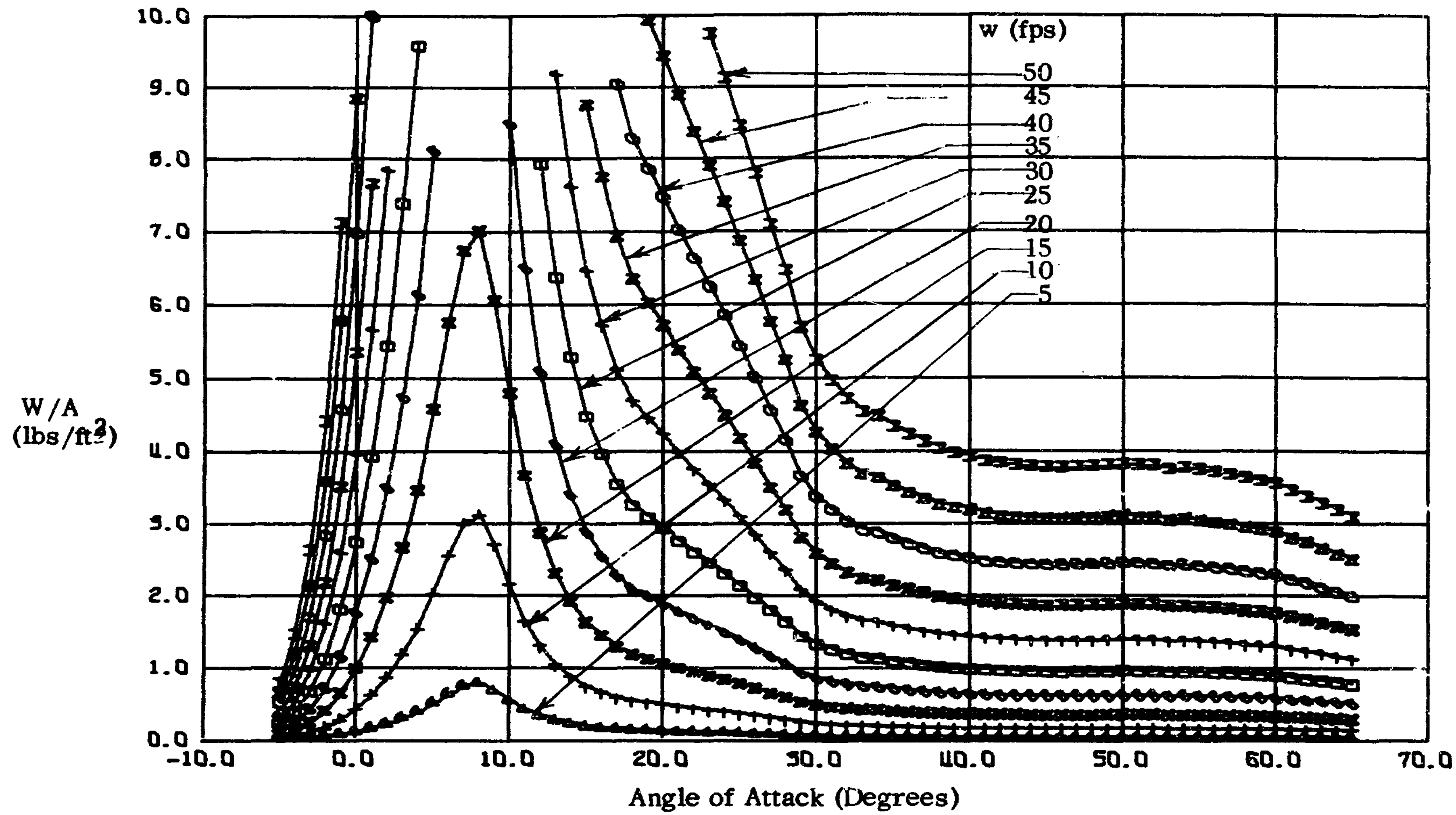

Figure I-18 Constant Rate of Sink Curves for Aspect Ratio 2.5 Parafoil

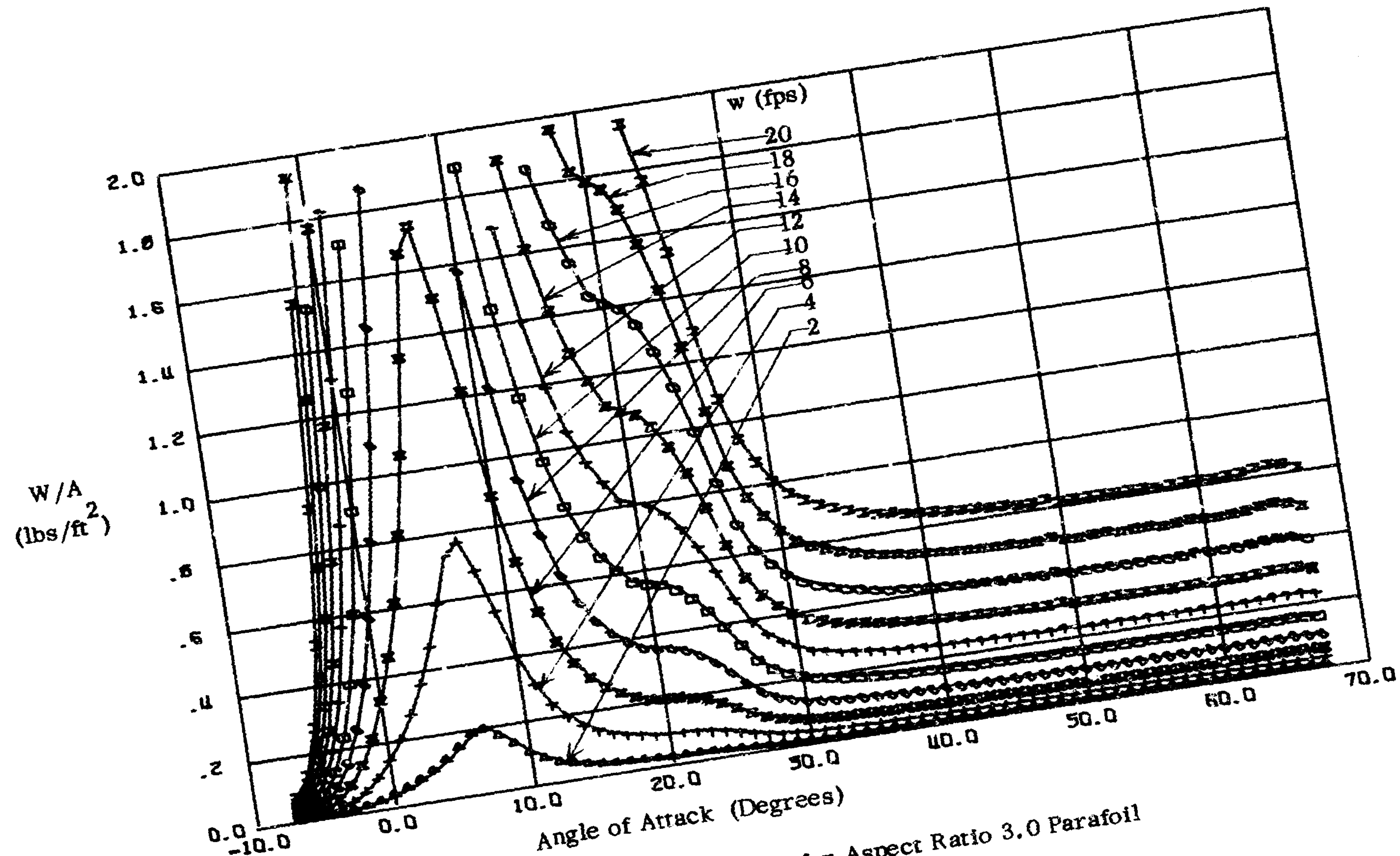

Figure I-14. Constant Rate of Sink Curves for Aspect Ratio 3.0 Parafoil

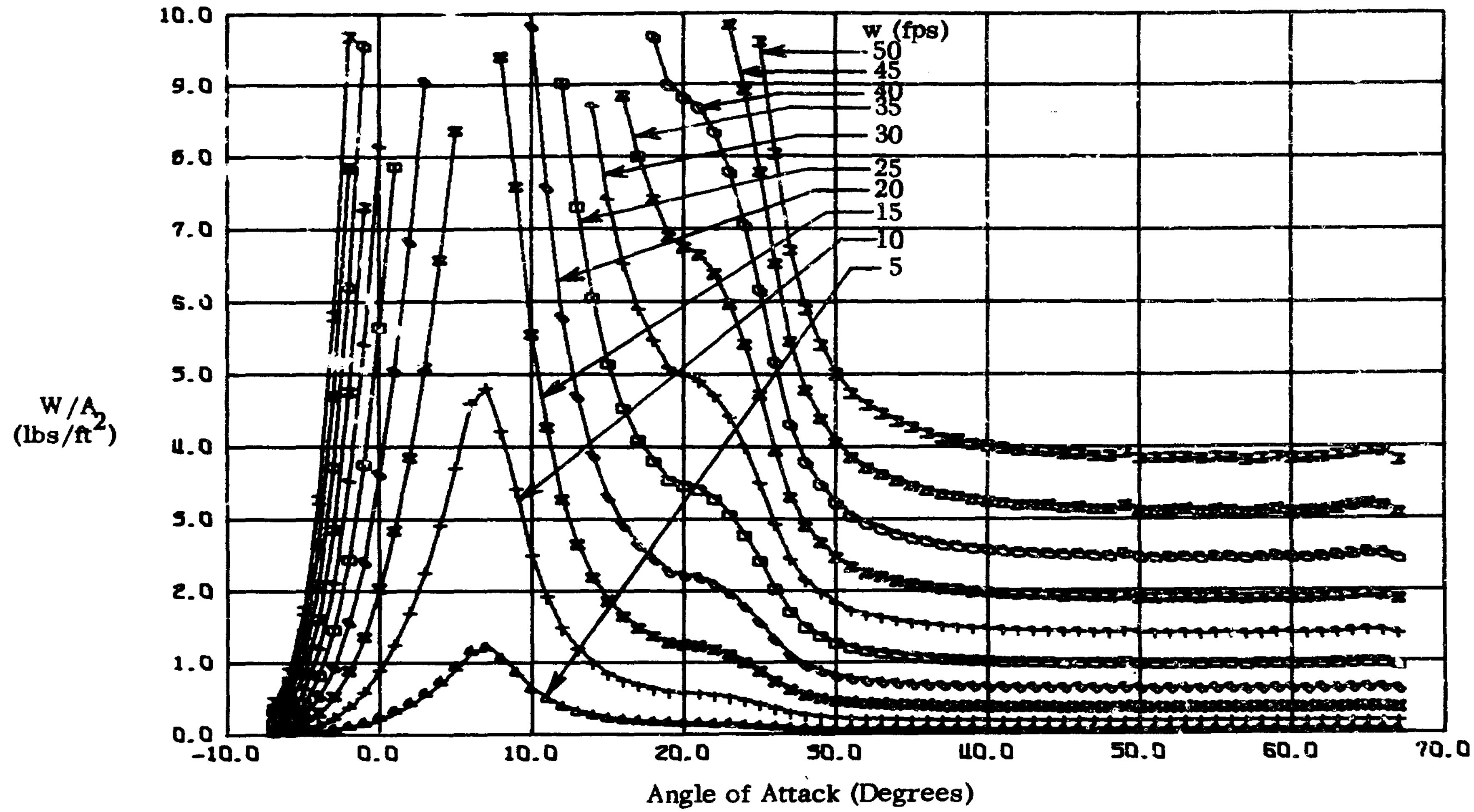

Figure I-15 Constant Rate of Sink Curves for Aspect Ratio 3.0 Parafoil

REFERENCES

1. Nicolaides, John D., and Knapp, Charles F., "A Preliminary Study of the Aerodynamic and Flight Performance of the Parafoil," AIAA 1st Conference on Aerodynamic Deceleration, University of Minnesota, July 8, 1965.

2. Nicolaides, John D., "On the Discovery and Research of the Parafoil," International Congress on Air Technology, Little Rock, Arkansas, November 1965.

3. Nicolaides, J.D., Knapp, C.F., "Para-Foil Design", University of Notre Dame Report (866). Prepared for the U.S. Air Force Flight Dynamics Laboratory, Wright-Patterson AFB, Ohio under Contract AF 33(615)-5004.

4. Knapp, C.F., and Barton, W.R., "Controlled Recovery of Payloads at Large Glide Distances, Using the Parafoil". Presented at the AIAA Sounding Rocket Vehicle Technology Specialist Conference, Williamsburg, Va., Feb. 1967; J. Aircraft, Vol. 5, No. 2; Sandia Laboratory SC-R-67-1049, under contract No. 48-2942, November 1967.

5. Nicolaides, J.D., "Summary Report on Parafoil Targetry", University of Notre Dame Report, 1968, prepared for the U.S. Air Force, Eglin Air Force Base, under Contract No. AF08(635)-6003.

6. Metres, Solomon R., et al. "Project Pin Point" Review Report, Air Force Flight Dynamics Laboratory, Director of Laboratories Air Force Systems Command, Wright Patterson Air Force Base, Ohio.*

7. Saar, J., LIFE, Sept. 1968.

8. Nicolaides, J.D., Speelman, R.J., Menard, G.L.C., "A Review of Para-Foil Programs", AIAA 2nd Aerodynamic Deceleration Systems Conference, El Centro, Calif., Sept. 1968.

9. Menard, George, "Performance Evaluation Tests, Parafoil Maneuverable Personnel Gliding Parachute Assembly Aspect Ratio 2, Area 360 sq. ft.", September 1969, Rpt. 2-69.

10. Nicolaides, J.D., "Improved Aeronautical Efficiency Through Packable Weightless Wings," CASI/AIAA Meeting on the Prospects for Improvement in Efficiency of Flight, Toronto, Canada, AIAA Paper No. 70-880, July 9-10, 1970.

11. Nicolaides, J.D., "Summary of Para-Foil Wind Tunnel Tests", University of Notre Dame report, 1969, prepared for the U.S. Flight Dynamics Laboratory, Wright Patterson AFB, Ohio under contract F33615-67-C-1670.

REFERENCES (continued)

12. Neumark, Walter, "Ascending Flight Technique", Manchester, England, 1970.

13. U. S. Army, Golden Knights Brochure, 1970.

14. Hoerner, Sighard F., "Fluid-Dynamic Drag". Published by the author, Midland Park, N.J. 1965.

*Reference 6 has been superseded by:

Speelman, R. J., et al. Para-Foil Steerable Parachute, Exploratory Development for Airdrop System Application. Air Force Flight Dynamics Laboratory Report, AFFDL-TR-71-37.

AIR FORCE: 20-9-71/280